Petroleum Source Rocks of Egypt: An Integrated Spatio-temporal Palynological and Organic Geochemical Studies Within the Phanerozoic

Haytham El Atfy, Bandar I. Ghassal, and Ralf Littke

Abstract

This chapter evaluates the integration between optical and geochemical methods as one of the best ways to screen hydrocarbon source rock potential and its diagnostic impact on kerogen investigation, in addition to its consistent involvement in paleoenvironmental inferences. While those kerogen types are usually resulting from Rock-Eval data, palynofacies and organic petrographic data deliver additional and consistent information. Rock-Eval data for samples with low to moderate TOC are mostly non-reliable due to free hydrocarbons in the mineral matrix. Consequently, palynofacies analysis represents a valuable complementary proxy for investigating the petroleum generation potential of source rocks. This chapter presents the first comprehensive review of the application of palynofacies with respect to the framework of geochemical data and the interpretations of different spatio-temporal source rock windows in Egypt. This integrated palynofacies and geochemical approach provides an improved understanding of the paleoenvironmental and petroleum source potential studies of the Phanerozoic sequences in Egypt.

Keywords

Petroleum source rocks • Palynology • Hydrocarbons • Kerogen • Palynofacies • Paleoenvironment • Phanerozoic

1 Introduction

Egypt possesses five primary petroleum provinces located in various geographical regions, namely the Gulf of Suez, Red Sea, Nile Delta, North Western Desert, and Southern Egypt. These provinces comprise prolific petroleum basins of diverse Phanerozoic ages (Fig. 1) and represent diverse depositional environments (e.g., passive margin, rift, terrestrial, deltaic, and marine). The variable geological settings and ages resulted in complex petroleum systems that have required detailed investigations by advanced techniques. Some of these basins are better understood due to a long exploration history, a large number of drilled wells, and the availability of geological, geochemical, and seismic data. Furthermore, some of the basins are poorly understood with respect to the depth and age of the intervals (e.g., below the best-known reservoir rocks), such as the pre-Miocene in the Nile Delta and the pre-Jurassic in the Western Desert. In addition, few attempts have been made to assess unconventional petroleum resources in spite of the presence of source rock outcrops in several areas.

This chapter provides detailed insights into the principal petroleum systems in Egypt. It also addresses the possible overlooked geological intervals which may be relevant to petroleum systems using in-depth comprehensive exploration techniques, mainly palynology and organic geochemistry. Palynology was widely utilized in the petroleum industry during the mid-twentieth century as a standard tool for exploration. Since the 1980s, palynology has not solely meant the study of spores, pollen, and other organic-walled microfossils. It encompasses investigations of all categories

H. El Atfy (✉)
Department of Geosciences, University of Tübingen, 72076 Tübingen, Germany
e-mail: El-Atfy@daad-alumni.de

Geology Department, Faculty of Science, Mansoura University, Mansoura, 35516, Egypt

B. I. Ghassal (✉)
Saudi Aramco, Dhahran, Saudi Arabia
e-mail: bandar.ghassal@aramco.com

R. Littke
Energy and Mineral Resources Group (EMR), Institute of Geology and Geochemistry of Petroleum and Coal, RWTH Aachen University, 52056 Aachen, Germany

Z. Hamimi et al. (eds.), *The Phanerozoic Geology and Natural Resources of Egypt*, Advances in Science, Technology & Innovation, https://doi.org/10.1007/978-3-030-95637-0_23

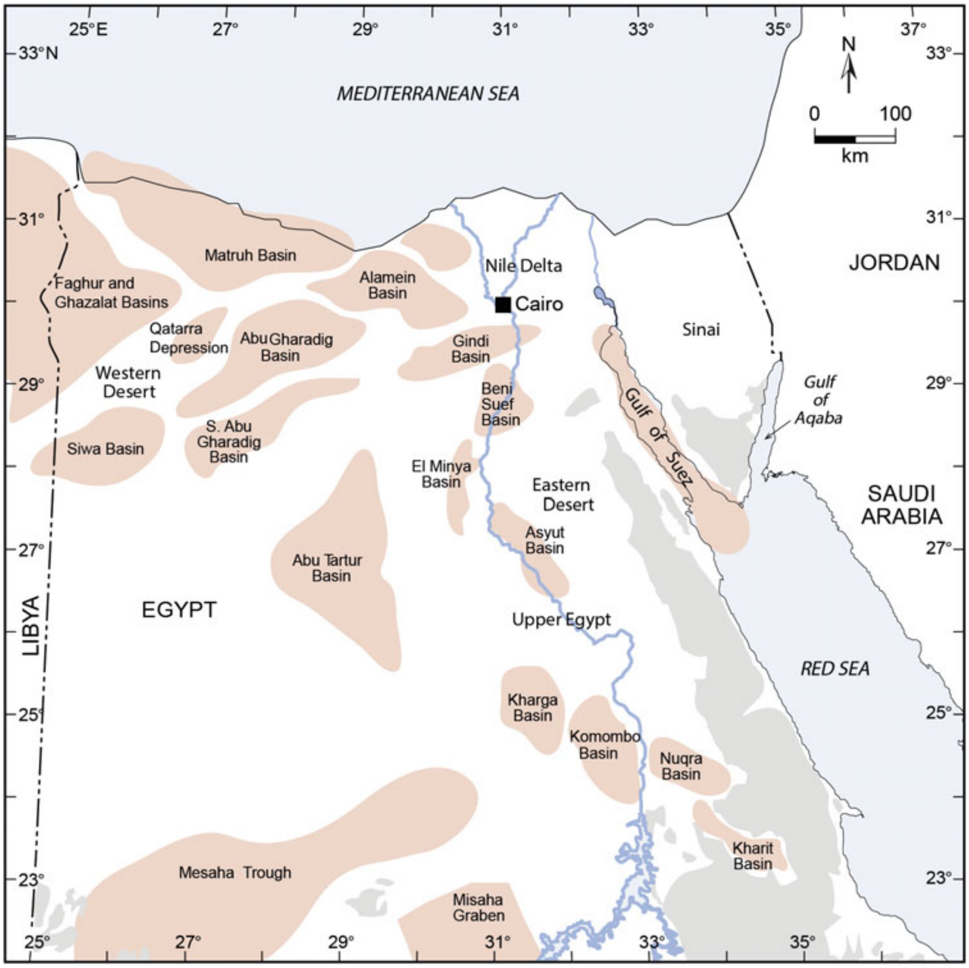

Fig. 1 Location map showing the sedimentary basins of Egypt (Dolson et al., 2000)

of microscopic organic particles ranging from objects with well-defined morphology, such as dinoflagellate cysts, wood particles and cuticles, structured and unstructured remains, and other tissues of indeterminate sources that are not easily categorized. Although palynology has a broad spectrum of applications in paleoenvironmental and paleoclimatic reconstructions, palynostratigraphy continues to be the most important for the majority of palynological research and is still the focus of most studies.

During the last few decades, more focus has been given to the wide variations in the composition of organic facies linked to different rock types, generating rapid growth of research in other non-biostratigraphic implications. The most important of these, because of their value to the petroleum industry, is the source rock evaluation in terms of quantity, quality, and maturation of organic matter (OM) recovered from sedimentary successions (Batten, 1982).

Palynofacies (sensu Combaz, 1964) analysis as a helpful proxy into the interpretation of depositional environments and petroleum source rock identification has been considered in detail by Tyson (1995) and Batten (1996a, 1996b), in addition to some more recent publications (e.g., El Atfy, 2021; Ghassal et al., 2018; Zobaa et al., 2013), thereby aiding in the general evaluation of the hydrocarbon potential. In the oil and gas industry, there is a considerable emphasis on improving the recovery of hydrocarbons within producing fields; thus, there is a need for biostratigraphy to be applied on a very fine scale to determine both the reservoir architecture and provide answers to problems associated with petroleum production and development. Under such circumstances, the palynological effort usually relies largely on quantitative and semi-quantitative analyses of data and, hence, on palynofacies analysis from which local changes in depositional conditions may be inferred (Batten, 1999).

Although some efforts have been made to integrate both palynological and sedimentologic data dating back to the 1950s, only within the last few years, has a substantial effort in these fields considering this sort of work thoughtfully. From the standpoint of petroleum potential, especially important studies should be concerned with the occurrence and composition of source rocks. Many papers have been written on this topic, but only a few discuss their palynological contents in satisfactory detail. The present chapter presents the first summary of the concept of palynofacies and its application within the context of geochemical data and interpretations of different spatio-temporal source rock windows in Egypt. Such an integrated approach undoubtedly enhances the understanding of the detailed paleoenvironmental and petroleum source potential studies in the Phanerozoic successions in Egypt.

It is also worth mentioning that, since the 1960s, researchers studying Egyptian palynology have focused on the classic aspects of palynology comprising taxonomy, palynostratigraphy, and paleoenvironmental deductions. Only recently have they started to give more consideration to the application of palynology for thermal maturation of organic constituents of sedimentary rocks (e.g., Hartkopf-Fröder et al., 2015) and source rock potential (El Atfy et al., 2014; Ghassal et al., 2018).

The integration between optical (i.e., palynofacies and organic petrology) and organic geochemical methods has a definite impact on determining kerogen types, petroleum source rock potential, and paleoenvironmental deductions. Kerogen types are traditionally assigned based on organic petrology and Rock-Eval pyrolysis. However, optical microscopic methods such as palynofacies and organic petrography can provide additional and reliable information. In particular, Rock-Eval pyrolysis data are mostly doubtful for samples with low to moderate TOC due to the retained hydrocarbons in the mineral matrix (e.g., Grohmann et al., 2018), in addition to unreliable readings of hydrogen and oxygen indices. Therefore, integrating geochemical and palynofacies methods is a valuable complementary technique for comprehensively investigating the petroleum generative potential of source rocks. Historically, this integration was first introduced for the Phanerozoic sediments in Egypt by El Beialy et al. (2010) for the Upper Cretaceous of the north Western Desert, followed by a series of contributions on different spatio-temporal stratigraphic windows, which will be discussed in depth subsequently in this chapter. The chapter employs integrated palynological and geochemical approaches to shed more light on selected case studies and examples and reviews the primary successions of the Phanerozoic sedimentary cover in Egypt.

2 Source Rock Deposition: Processes and Mechanisms

Source rocks are fine-grained carbonate or siliciclastic sedimentary rocks that are rich in organic matter and expected to generate hydrocarbons when subjected to high temperatures (Littke et al., 1997; Tissot & Welte, 1984). Organic matter productivity, preservation, and depositional settings are the key aspects that control the source rock richness and quality (Ghassal, 2017). The origin of the organic matter in source rocks is either transported (allochthonous), mostly from terrestrial sources, or in-situ (autochthonous), (e.g., Bustin, 1988; Katz, 2012; Littke et al., 1997). Comprehensive investigations have been conducted to understand the productivity and preservation of organic matter, as well as kerogen formation under several depositional environmental conditions. This section reviews the common marine source rock depositional environments that mostly characterize the Egyptian source rocks.

The Nile Delta petroleum system represents one of the most challenging systems investigated in Egypt (Ghassal et al., 2016), especially because the depositional environment of deltas is transitional from terrestrial to marine settings. Deltas are characterized by high energy and sedimentation rates, the predominance of silicates, and the presence of abundant heavy minerals within low salinity waters (Ghassal, 2017). In such fluvial-deltaic settings, higher land plant tissues are common with a lower content of aquatic algae (Bustin, 1988; Littke et al., 1997; Tissot & Welte, 1984). Galloway (1975) classified deltaic environments into three chief types: river-dominated, wave-dominated, and tide-dominated deltas—primarily based on the supply and types of sediments. In addition, primary productivity and organic matter preservation are significantly different in these three types of deltas. Prominent examples of river-dominated petroleum systems are the Mississippi, Niger, and Mahakam deltas (e.g., Peters et al., 2000; Tuttle et al., 1999). Therefore, this delta type is probably the most well-understood system among the three types in terms of petroleum potential. However, the Nile Delta which is allocated as a wave-dominated delta (Coe et al., 2003), is still poorly understood (Ghassal et al., 2016). Rivers supply the inner shelf with terrestrial organic matter such as vitrinite, inertinite, and coal particles as well as fresh/brackish water algae (Ghassal, 2017; Ghassal et al., 2016). Mixing of freshwater and marine water can lead to changes in nutrient supply and thus primary productivity and bottom water oxygen supply. Moreover, the liptinite macerals possess low densities that make them selectively transported (Bustin, 1988). These effects lessen toward the distal settings as the interplay between fluvial and marine systems becomes minimal. Other factors such as tectonism, climate, and sea-level change play significant roles in the bottom water condition and, thus, the source rock quality and richness.

Rift basins usually host prolific petroleum source rocks in the pre-, syn- and post-rift sections. Typical examples are the Atlantic Ocean and Red Sea basins (e.g., Duarte et al., 2012; Ghassal, 2010; Katz, 1995). Small rift basins and failed rift basins also host source rocks but on a small scale, depending on the burial history, dimensions of the basin, sedimentation rates, and climate (Katz, 1995). Due to the tectonic complexities and rapid changes in sediment fill and water chemistry in such basins, the source rock distribution, richness, quality, and thermal maturity are very heterogeneous within small distances (Ghassal, 2010; Katz, 1995). Note that there are two types of rift systems: marine and non-marine basins. The focus of this chapter is on the marine rift system as it represents the common type found in the various Egyptian basins (the Gulf of Suez Basin is the prominent example). In rift basins, the balance between primary productivity and preservation is the principal controlling factor of the source rock richness. These two factors are regulated by tectonic stability and sedimentation rates which change the oxygen contents and drive the nutrient availabilities (Katz, 1995 and references therein).

Apart from rift basins, sedimentation of marine petroleum source rocks occurs mainly in three settings, namely oxygen minimum zones on continental margins, upwelling zones, and silled/barred basins (Fig. 2) (e.g., Katz, 2012; Littke, 1993; Selley, 1998).

The biomass decay and the deficiency of circulation and photosynthesis in relatively deep and dark water consume the bottom water oxygen and inhibit its resupply, which causes anoxic conditions and creates oxygen minimum zones (Selley, 1998). Furthermore, water temperature and salinity determine the position of these zones (Katz, 2012). Upwelling zones reckon nearly half of the organic-rich source rocks worldwide (Parrish, 1987) and are characterized by high biological productivity that surpasses the productivity of regular shelves by almost three-fold (Katz, 2012; Koblentz-Mishke et al., 1970; Ryther, 1969). During the predominant global greenhouse warming climate, winds move the shallow coastal warm water, which enables upwelling nutrient-rich water to substitute it (Bakun, 1990). The introduction of the nutrients increases bio-productivity, and later rapid deposition of organic matter (Bakun, 1990; Parrish, 1987). Additionally, the water oxygen level decreases, creating favorable conditions for organic matter preservation (Katz, 2012; Parrish, 1987). Climate also plays a significant role in intensifying the upwelling processes that are less prevailing during cold phases (Bakun, 1990; Parrish, 1987). Furthermore, the locations of the pronounced upwelling zones are usually along the western continental margins due to variations in wind direction and the Coriolis Effect ensuing from Earth's rotation (e.g., Katz, 2012).

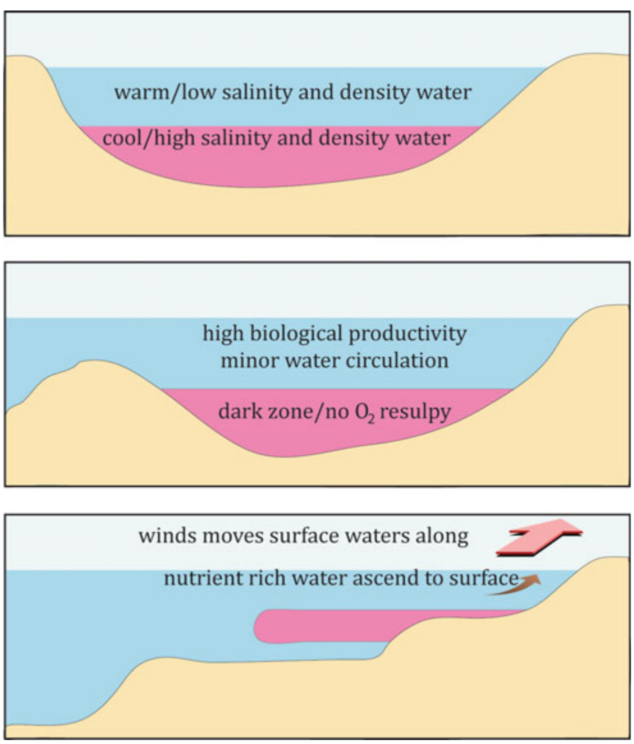

Fig. 2 A schematic diagram of common marine source rock depositional settings. Pink polygons are anoxic/oxygen minimum zones

In silled/barred basins, the bottom water anoxia evolves due to density-related stratification or thermal stratification. Density stratification forms when low saline and less dense water cover the more saline and denser deep water. Thermal stratification occurs when warm water rests on colder ones and no mixing takes place. Many barred basins are present in tropical and subtropical areas where minimum changes occur in the seasonal temperatures (Gluyas & Swarbrick, 2013; Katz, 2012).

3 Source Rock Distribution Through Time and Space—Egyptian Outlook

The Paleozoic source rocks in Egypt are poorly understood due to limited well penetrations and outcrop data. A generic overview of the geology and available source rock understanding is discussed in this section. Moreover, a global-scale glaciation event took place through the stabilization of the Gondwana supercontinent (~750–600) (Craig et al., 2009). There is no evidence of Infra-Cambrian source rock potential in Egyptian basins due to the lack of suitable climatic, tectonic, and marine and non-marine source rock development conditions (Bassett, 2009; Craig et al., 2009; Lučić and Bosworth 2019). Throughout the Paleozoic, a significant part of North Africa acted as the southern margin of the paleo-Tethys ocean, which received sediments from the hinterland from the south (Lučić and Bosworth 2019). The Paleozoic witnessed four global-scale glaciation events alternating with multiple marine transgressions, which resulted in siliciclastic-dominated tectonostratigraphy (Bassett, 2009; Beydoun, 1998; Craig et al., 2009; Lučić and Bosworth 2019). The lower Silurian hot shales constitute a major domain of the proven Paleozoic source rocks in northern Africa. These shales, which are rich in organic matter and uranium, are primary source rocks in North Africa and Arabia (Abohajar et al., 2015; Abu-Ali and

Littke 2005; Belaid et al., 2010; Dolson et al., 2014; Lüning et al., 2000; Yahi et al., 2001). However, these successions have not been discovered in Egypt yet. Few studies reported siltstone dominated lithologies in various locations in Egypt but no organic-rich layers (El-Hawat et al., 1997; Keeley, 1989; Klitzsch, 1990; Lüning et al., 2000).

The source rock deposition of the Mesozoic to Cenozoic in Egypt was controlled by several tectonic and climatic events including the breakup of Gondwana, Jurassic rifting, the Red Sea opening, the Syrian Arc event, and the Messinian Salinity Crisis. Moreover, several global warming/cooling climatic phases prevailed, which triggered oceanic anoxic events and intensified the sea-level changes.

The extensional system in North Africa, in general, is largely attributed to the opening of the Central Atlantic and the drift of the Turkish-Apulian terrain (Guiraud et al., 1987). During the Middle Jurassic, East–West half-graben evolution occurred in an association with sea-level transgressions. Prolific source rock depositions span the Middle Jurassic, such as the Masajid Formation. However, some of these source rock successions were eroded throughout the Upper Cretaceous and Cenozoic inversions (Guiraud & Bosworth, 1999). Good to excellent source rock potential with variable qualities occurs in rocks in the Gulf of Suez, southern Nile Delta, and the Western Desert (see details in Sect. 4).

During the Early Cretaceous, active rifting occurred coevally with the separation of the Arabian-Nubian Block from the South American Plate (Guiraud et al., 2005). Rifting continued during the Aptian until the Santonian. Furthermore, warm climate and the highest recorded Phanerozoic sea transgressions occurred throughout the Middle to Late Cretaceous, which resulted in oceanic anoxic events (OAEs) (Berra & Angiolini, 2014; Guiraud et al., 2005; Haq et al., 1988). The OAEs represented periods of excessive organic carbon deposition and improved bottom water anoxia (Jenkyns, 2010). The best source rock quality intervals in Egypt were deposited during the Cretaceous in all the major Egyptian petroleum basins (e.g., El Atfy et al., 2019; Ghassal et al., 2018).

Large areas of North Africa witnessed major sea transgression during the Paleocene to Eocene, which was responsible for depositing shallow marine sediments (Guiraud et al., 2005). During the early Oligocene, high sea level coexisted with the NE-SW extensions in North Egypt, which started the Gulf of Suez and the Red Sea rifts (Dolson et al., 2014).

During the Miocene, extreme compressional and extensional tectonic events prevailed in Northeast Africa, including the rifting of the Red Sea and the Gulf of Aqaba, and the maturation of the River Nile (Bosworth et al., 2005; Dolson 2020). The Miocene witnessed the deposition of the primary source rocks in the Nile Delta, Gulf of Suez, and the Red Sea basins (El Atfy et al., 2014; Ghassal et al., 2016). The Quaternary is characterized by extensive fluvial deposits (Guiraud et al., 2005). No source rock deposition was recognized during this time.

4 Phanerozoic Source Rocks—Examples and Evaluation

4.1 Paleozoic Source Rocks

The oldest recognized potential source rocks in Egypt are in the poorly studied Carboniferous basins in the Western Desert that are unseen underneath the Hercynian unconformity and, consequently, poorly understood. To the west, in Libya and Algeria, sub-Hercynian traps comprise stratigraphic and structural cessations often sourced by bulky glacially scoured valleys that were later infilled with Silurian and Devonian source rocks. It is possible that comparable settings occur across northern Egypt, but they have not been proven so far from seismic and well data (Dolson 2020 and citations therein).

To the authors' knowledge, the only published studies on the palynofacies of the Paleozoic of Egypt have been by Makled et al., (2018, 2021). They integrated palynofacies with Rock-Eval pyrolysis and organic petrography to assess the hydrocarbon generation potential of the Devonian strata within the Faghur-1, NWD-302–1, and Sifa-1X wells in the north Western Desert. Their palynofacies data generally revealed the occurrence of gas-prone kerogen Type III. TOC concentrations indicate poor organic richness with content not exceeding 0.9 wt.%. These sediments are mostly mature based on the TAI (2–3). Their burial history models showed that hydrocarbon generation started throughout the Cretaceous in the studied boreholes. From our perspective, the T_{max} and Production Index (PI) data are not reliable in this case due to the low quality and insufficient reactive kerogen contents. Moreover, the reported TOC values indicate insignificant volumes of generated hydrocarbon.

However, in their study of the Sifa-1X well, Makled et al. (2021) reveal that Devonian succession has organic matter content of varied kerogen, namely Type I, Type II, mixed types II/III, and Type III. This mixture of kerogen was also identified using organic elemental and pyrolysis gas chromatography data. Furthermore, maturity data from the well shows that the entire Devonian sequence belongs to the oil window, and hence, has the potential to generate oil and gas.

4.2 Mesozoic Source Rocks

4.2.1 North Western Desert

Within the north Western Desert, the Upper Jurassic-Lower Cretaceous sequences are among the most prolific hydrocarbon plays in North Africa. Though, their source rock characteristics and depositional environments are still not well known (El Atfy et al., 2019). Palynologically, those subsurface Jurassic-Cretaceous strata were the subject of several palynological investigations that have chiefly focused on taxonomy, palynostratigraphy, and to a lesser extent paleoenvironmental interpretations. On the other hand, few efforts have been paid to examine the thermal maturity and source rock potential (e.g., Ibrahim et al., 1997; El Beialy et al., 2010 and references therein; Zobaa et al., 2013; Ghassal et al., 2018; Gentzis et al., 2018; El Atfy et al., 2019).

(a) **Jurassic**

Felestteen et al. (2014) introduced the first comprehensive palynofacies investigation supplemented with organic geochemistry that targeted the Jurassic deposits in the north Western Desert. However, a previous investigation carried out on the Masajid Formation by Zobaa et al. (2013) produced relatively similar palynofacies results, as was also the case for the studies by Hewaidy et al. (2014) and El Atfy et al. (2019). The palynofacies results of Felestteen et al. (2014) did not offer a clear separation between the different Jurassic rock units, resulting in their being lumped under one palynofacies group dominated by opaque phytoclasts and interpreted as mixed but gas-prone facies. El Atfy et al. (2019) suggest fair to good gas source rock potential, with possible minor oil potential within multiple intervals in the Jurassic formations (Fig. 3). Their TOC concentrations exceed 2.0 wt.% and HI values reach 240 mgHC/gTOC. The results of Felestteen et al. (2014) share the same conclusions. They reported marginal to very good source rocks with TOC and HI values up to 4.0 wt.% and 199 mgHC/gTOC, respectively, at low thermal maturity.

Gentzis et al. (2018) studied the hydrocarbon potential of the Jurassic succession in the Abu Tunis-1 × well in the Matruh Basin, north Western Desert. Their multi-proxy approach identified two palynofacies associations for the studied material, both are AOM-dominated. The first association represented the Wadi Natrun Formation, the lowermost and the uppermost Khatatba Formation, and the Masajid Formation. The second palynofacies association from the upper Khatatba Formation. The Rock-Eval and organic petrological data reveal similar conclusions with relatively high TOC and HI index values and VRe values exceeding 0.9%. The evaluated Jurassic section possesses mixed Type II/III kerogen and attained thermal maturity within the peak oil window.

A recent investigation of the Khatatba and uppermost Ras Qattara formations in the Falak-21 borehole (Shushan Basin) by Mansour et al. (2020) tells that this interval has a good–excellent generative potential (kerogen Type III). The maturity reached a mature oil window in the Khatatba and uppermost Ras Qattara formations. Based on the total sulfur (TS) versus TOC relationship, the uppermost Ras Qattara Formation and Yakout Member (of the Khatatba Formation) were formed under oxic circumstances, however, the middle and upper parts of the Khatatba Formation were mostly deposited throughout high paleoproductivity in dysoxic–suboxic and suboxic conditions, correspondingly.

(b) **Cretaceous**

The Cretaceous strata in Egypt comprise manifold generative source/reservoir intervals. Consequently, they are considered the chief deeply-seated exploration goals of working companies, especially in the north Western Desert. A closer view of the Cretaceous sedimentary successions demonstrates that they have been well explored in comparison with the pre- and post-Cretaceous layers. The Cretaceous strata in the north Western Desert are subdivided into a lower unit, made of clastics that have their place in the Lower Cretaceous Burg El Arab Formation (comprising from bottom to top: Alam El Bueib, Alamein, Dahab, and Kharita members), and an upper unit composed of carbonates of Upper Cretaceous age that represent from bottom to top, the Bahariya, Abu Roash, and Khoman formations.

Lower Cretaceous

In spite of the fact that the Upper Jurassic-Lower Cretaceous sequences in the north Western Desert are among the most productive hydrocarbon plays in North Africa, their source rock characteristics and depositional environments are still not well known. The study of El Atfy et al. (2019) which utilized an integrated palynofacies and organic geochemical approach for the Upper Jurassic Masajid Formation and Lower Cretaceous Alamein and Alam El Bueib members in the OBA. 3–1/1A and OBA. S-C wells yielded interesting results (Fig. 3). Two main organic facies types connected to depositional environments and kerogen types were established: palynofacies PF I in the Alamein and Alam El Bueib members and PF-II in the Masajid Formation. PF I is expressed by kerogen Type II and Type III, which is more confirmed by pyrolysis data that tell fair organic richness and gas generation potential in the Alamein Member, with TOC values ranging from 1.0 to 2.5 wt.% and HI from 64 to 112 mg HC/gTOC. The Alam El Bueib Member demonstrated better organic richness and quality with TOC ranging from 1.6 to 3.1 wt.% and HI from 121 to 318 mg HC/gTOC. The thermal maturity assessment indicates that the Alamein Member is immature, whereas the Alam El Bueib Member is early to oil-mature (Table 1). Furthermore, the APP ternary

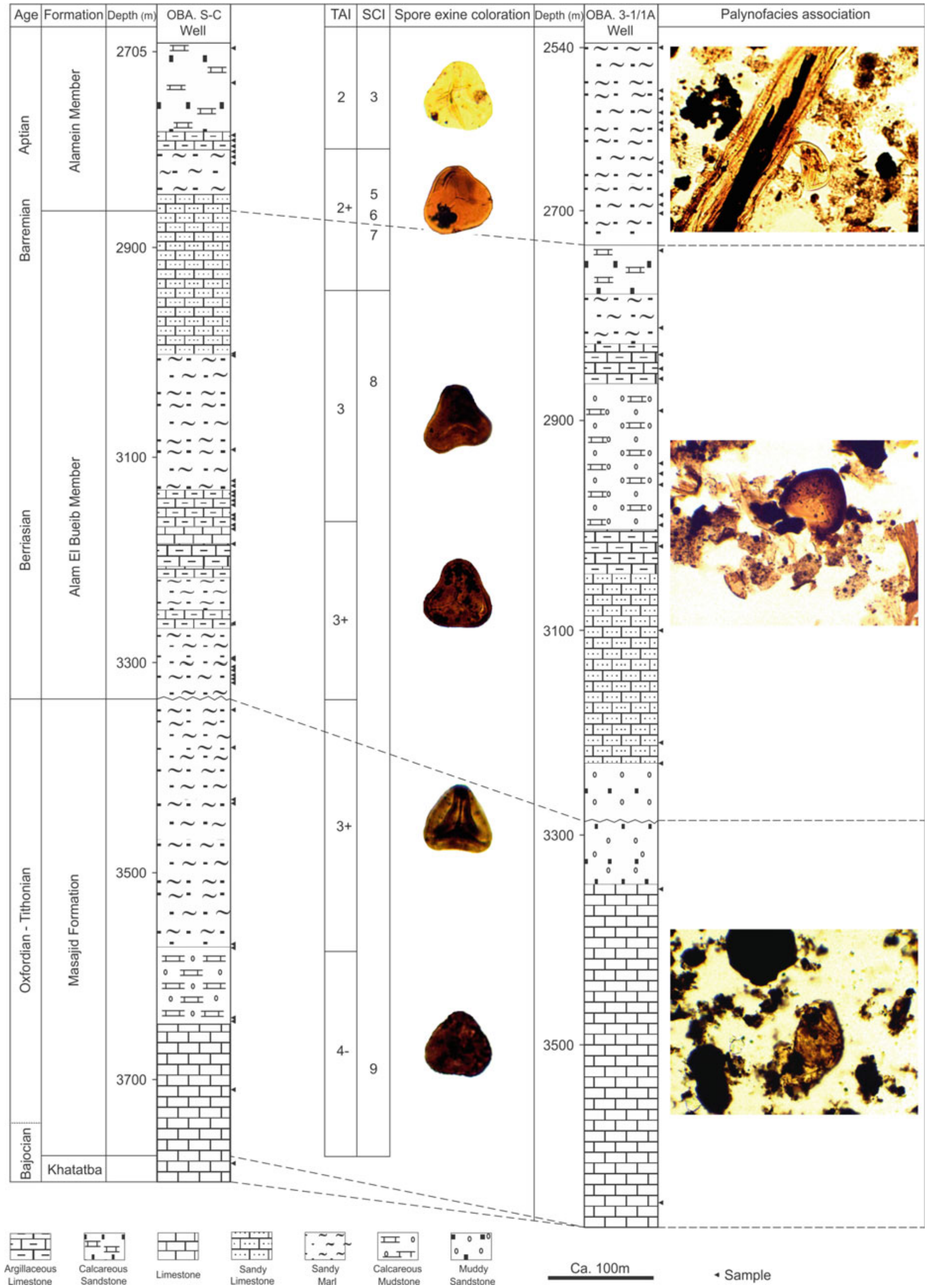

Fig. 3 Palynofacies, TAI, and SCI readings of the upper Jurassic-lower Cretaceous samples (BA. 3-1/1A and OBA. S-C wells), north Western Desert, Egypt (El Atfy et al., 2019). Spore colors follow the corrected scheme of Pearson (1984); SCI numbers per Marshall and Yule (1999) and TAI numbers after Batten (1982)

plot data suggest that both the Alamein and Alam El Bueib members were formed in a suboxic to anoxic basin (Fig. 4). While the Type III kerogen (gas-prone) interpretation for the Alamein Member by El Atfy et al. (2019) is similar to those previously described for the Sharib-1 × and Ghoroud-1 × wells (Zobaa et al., 2013), other authors, such as Ibrahim et al. (1997) and El-Soughier et al. (2010) stated that the Alamein Member was characterized by Type II kerogen (oil-prone).

It is worth noting here that the Late Jurassic and Early Cretaceous perceived the deposition of gas-prone source rocks as similar to those from the southern onshore Nile Delta Basin. These results have weighty inferences for the understanding of the types of source rocks in the northern onshore and offshore Egyptian basins and the future of gas exploration in the region (El Atfy et al., 2019). These source rock intervals were deposited in shallow marine environments based on geochemical and palynological assessments. Better source rock qualities are expected in deeper facies where optimum preservation of organic matter prevailed, but more work is needed to completely understand the source rock quality and distribution in this vital petroleum basin.

Upper Cretaceous

The integrated approach for studying the Upper Cretaceous successions in the north Western Desert was pioneered by El Beialy et al. (2010), who studied the subsurface Cretaceous units in the basin through a collective optical (spore coloration, palynofacies, and vitrinite reflectance) and organic geochemical (TOC and Rock-Eval pyrolysis) investigation. Their results appear to be valid for most north Western Desert regions and have been confirmed by other later contributions, such as Zobaa et al. (2011) and Mahmoud et al. (2017). In a detailed study, Ghassal et al. (2018) refined the results of these earlier studies to provide new understandings of the depositional environment from the Cenomanian to the Santonian (Table 2; Fig. 5), as well as the petroleum source rock potential of the Abu Roash "*F*" Member and residual hydrocarbons in the Abu Roash "*C*" and "*D*" members. Below, we highlight the results from all these studies.

1. The Abu Roash and Bahariya formations are comprised mainly of kerogen Type III, and thus gas-prone, except for the Abu Roash "*F*" Member which shows of an oil-prone facies (Fig. 6).
2. In contrast to the other Abu Roash members, the "*F*" Member shows a positive correlation between TOC and $CaCO_3$ as well as TS. It signifies an interval of anoxic or strongly oxygen-depleted bottom waters with improved preservation of organic matter, which is expressed in a high proportion of amorphous organic matter (AOM), high TOC, and HI values. This organic-rich layer is interpreted to mark the short-term global oceanic anoxic event (OAE2). Three depositional phases (Figs. 7 and 8) have been recognized, as follows:
   a. Transgression phase-I is marked by anoxic bottom water conditions, generating sediments that are rich in TOC, carbonate, and S, and partially deprived in Fe and other detrital elements. This recommended sulfur amalgamation into organic matter. Sediments representing this phase seem to have been deposited in a more humid climate compared to the other intervals based on the illite/smectite ratio.
   b. Regression phase has seen a fall in sea level and freshwater incursions, together with acidification of the waters and heavy mineral deposition, as construed from the abundance of siderite, rutile, detrital elements, and Mn.
   c. Transgression phase-II is plentiful in TOC, characterized by suboxic conditions and fairly higher detrital element concentrations related to transgression phase-I, which hampered sulfur assimilation into kerogen.
3. The differences between the two transgressive phases of the depositional environment resulted in the formation of types of two source rocks, one, as well as the other, is immature relative to oil generative potential. Nevertheless, transgression phase-I source rock comprises kerogen Type IIS, which produces high sulfur oil, whereas transgression phase-II contains kerogen Type II/III, which expells sweet oil with negligible gas upon expulsion. Interestingly, Rock-Eval and biomarker maturity data reveal lower thermal maturity for the Abu Roash "*F*" source rock interval compared to the sediments beyond it. This conclusion advocates retardation/suppression of maturation courses in oil-prone source rocks, but may also be due to the existence of migrated bitumen of improved maturity, i.e., from deeper source rocks, in all rock units except for the Abu Roash "*F*" Member.
4. The residual oils of the Abu Roash "*C*" and "*D*" reservoirs reveal two different partitions. The Abu Roash "*D*" residual oils are forced by either biodegradation or evaporation, whereas those from the Abu Roash "*C*" show a bi-modal *n*-alkane distribution with higher concentrations of low molecular hydrocarbons relative to the Abu Rash "*D*" residual oils. The different oil types may be indicative of more than one source rock charging the Abu Roash Formation.
5. Quantitative and qualitative investigations of palynofloras and palynofacies show that the Abu Roash "*A*" and "*C*" Members, together of Coniacian-Santonian age,

Table 1 TOC and rock-eval pyrolysis results of the upper Jurassic-lower Cretaceous samples (OBA. 3-1/1A and OBA. S-C wells), north Western Desert, Egypt (El Atfy et al., 2019)

Sample	Well	Rock unit	Depth (m)	Petroleum potential		Kerogen quality		Thermal maturity		OI (mg CO_2/g rock)	PI	S_2/S_3	TIC (wt. %)	$CaCO_3$ (wt. %)
				TOC (wt. %)	S_1 (mg HC/g rock)	S_2 (mg HC/g rock)	S_3 (mg CO_2/g rock)	HI (mg HC/g TOC)	T_{max} (corr.)					
15/1321	OBA. 3-1/1A	Alamein member	2582	1.04	0.12	0.67	0.96	65	429	93	–	0.70	7.04	58.63
15/1327	OBA. 3-1/1A	Alam El Bueib member	2860	–	7.85	3.39	0.27	–	–	–	–	–	–	–
Ex1				2.11	0.27	2.55	4.00	121	427	190	0.09	0.64	0.13	1.08
15/1328	OBA. 3-1/1A	Alam El Bueib member	3100	–	20.56	10.50	0.21	–	–	–	–	–	–	–
Ex1				–	0.45	7.10	1.33	–	436	–	0.06	–	–	–
Ex2				2.06	0.26	6.27	0.94	304	437	45	0.04	6.69	0.09	0.71
15/1329	OBA. 3-1/1A	Alam El Bueib member	3210	–	28.63	15.48	0.21	–	–	–	–	–	–	–
Ex1				–	–	–	–	–	–	–	–	–	–	–
Ex2				3.01	0.24	9.59	1.41	319	437	47	0.02	6.83	0.06	0.51
15/1330	OBA. 3-1/1A	Alam El Bueib member	3250-	–	28.13	12.01	0.21	–	430	–	–	–	–	–
Ex1				–	0.55	6.46	1.77	–	–	–	–	–	–	–
Ex2				2.25	0.15	4.92	1.27	218	434	56	0.03	3.87	1.19	9.95
15/1331	OBA. 3-1/1A	Masajid formation	3400	–	23.56	0.20	–	–	–	–	–	–	–	–
Ex1				2.40	0.52	5.65	1.81	236	427	75	0.08	3.13	1.82	15.14
15/1343	OBA. S-C	Alamein member	2740	–	2.96	3.41	0.24	–	429	–	–	–	–	–
Ex1				–	0.14	2.82	2.15	–	433	–	–	–	–	–
Ex2				2.50	0.19	2.85	1.94	113	433	77	0.06	1.46	2.73	22.76
15/1350	OBA. S-C	Alamein member	2800	–	1.22	2.11	0.19	–	–	–	–	–	–	–
Ex1				–	0.07	1.35	1.71	–	–	–	–	–	–	–
Ex2				2.04	0.08	1.46	1.34	71	433	66	0.05	1.09	0.60	4.98
15/1352	OBA. S-C	Alam El Bueib member	3002	–	3.22	5.85	0.21	–	434	–	–	–	–	–
Ex1				2.89	0.18	5.10	2.10	176	436	72	0.03	–	2.30	19.18
15/1353	OBA. S-C	Alam El Bueib member	3160	–	3.85	5.33	0.21	–	432	–	–	–	–	–
Ex1				–	0.19	3.90	2.33	–	434	–	–	–	–	–
Ex2				2.76	0.09	3.53	1.99	128	434	72	0.03	1.78	0.03	0.25
15/1357	OBA. S-C	Alam El Bueib member	3314	–	2.95	4.10	0.25		428	–	–	–	–	–
Ex1				1.54	0.10	2.79	1.02	181	435	66	0.03	2.75	0.24	1.99
15/1360	OBA. S-C	Masajid formation	3572	–	3.79	5.87	0.25	–	–	–	–	–	–	–
Ex1				1.28	0.08	1.89	0.87	148	430	68	0.04	2.17	2.60	21.96
15/1362	OBA. S-C	Khatatba formation	3782	2.43	0.36	5.80	2.42	239	431	100	0.06	2.40	3.71	30.92

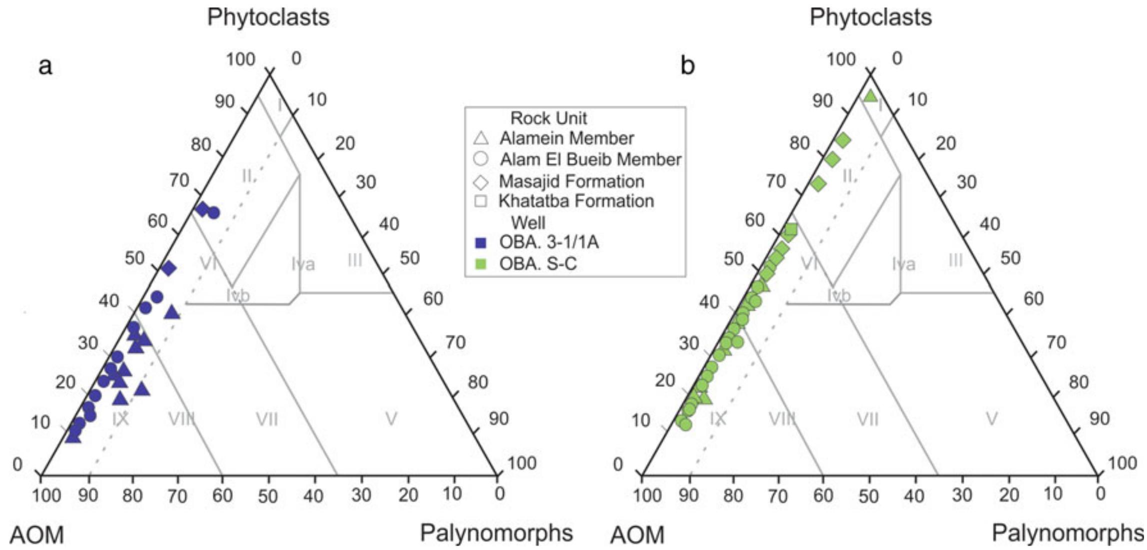

Fig. 4 APP ternary plot (Tyson 1993), A = OBA. 3-1/1A well, and B = OBA. S-C well. Field I = kerogen type III; field II = kerogen type III; field III = kerogen type III or VI; field IV = kerogen type III or II; field V = kerogen type III>IV; field VI = kerogen type II; field VII = kerogen type II; field VIII = kerogen type II>I

signify an oxic proximal and distal shelf environments, respectively. The Abu Roash "*D*" and "*E*" members, dated as Turonian, denote an oxic proximal shelf, whereas the Abu Roash "*F*" Member of the Cenomanian age was deposited in a distal suboxic–anoxic basin. The Abu Roash "*G*" Member and the Bahariya Formation, also Cenomanian in age, were formed in shallow marine and shallow marine to fluvio-deltaic environments, correspondingly. The integrated approach illustrates strong agreement between the palynological, organic, and inorganic geochemical interpretations.

4.2.2 Gulf of Suez

Petroleum exploration in the Gulf of Suez is relatively difficult since it is surrounded by many uncertainties. Due to huge sequences of evaporites, seismic data for the pre-salt are of very limited use and much of the Rock-Eval data are missing or unreliable. As discussed earlier, rift basins are very dynamic, and hence, the source rock quality, thickness, and distribution are highly variable. Also, approximately, all organic-rich intervals in the Gulf of Suez are drained in humic macerals while vitrinite particles are mostly absent, or show low reflectance (Mostafa & Ganz, 1990). Therefore, introducing palynofacies as an exploration tool, especially as a maturation detection parameter, will help to solve this problem.

El Diasty et al. (2014) introduced the first combined palynofacies and organic geochemical study that focused on the Upper Cretaceous-Eocene (Matulla, Brown Limestone, and Thebes formations) within the central part of the Gulf of Suez. Palynofacies analysis (Fig. 9) indicated that the Thebes and Brown Limestone formations were both deposited under a distal suboxic–anoxic environment. Conversely, the Turonian-Santonian Matulla Formation supports the presence of variable depositional settings from a marginal marine under dysoxic–anoxic basinal to proximal suboxic–anoxic shelf environments. Rock-Eval pyrolysis and TOC results indicate that most of the formations are immature to slightly mature and have a good petroleum source potential. They are organic-rich, containing oil- and gas-prone Type II and III kerogens, preserved under marine reducing conditions satisfactory for hydrocarbon generation and expulsion.

4.2.3 Nile Delta

The Nile Delta Basin is well-thought-out one of the most prolific petroleum basins in Egypt and the eastern Mediterranean region, particularly for gas resources, and accounts for approximately 60,000 km^2 correspondingly onshore and offshore (Barakat, 2010).

Data for the source rocks within the Mesozoic strata in the Nile Delta Basin (sometimes referred to as the north Eastern Desert) based on an optical investigation (i.e., palynofacies) are available exclusively from Ibrahim et al. (1997). They applied the spore coloration index (SCI), which is equivalent to the thermal alteration index (TAI), in an attempt to deduce the thermal maturation of the sediments. They inferred that the Jurassic sequence in the Abu Hammad-1 well was generally thermally mature, while the overlying Lower Cretaceous sediments were immature. In their conclusion, Ibrahim et al. (1997) highlighted the

Table 2 Carbon, sulfur, and rock-eval data of the upper Cretaceous Bahariya and Abu Roash formations (GPT-3 well), north Western Desert, Egypt (Ghassal et al., 2018)

Sample no.	Sample type	Depth (m)	Formation	TOC (%)	CaCO3 (%) ^	TS (%)	*S1**	*S2* *	*S3***	T_{max}***	PI	HI ****	OI *****
15/400	Cuttings	1413–1416	Abu Roash "*A*"	1.30	26.50	1.13	0.12	1.06	3.25	431	0.10	82	249
15/401	Cuttings	1422–1425	Abu Roash "*A*"	1.25	33.10		0.11	0.85	2.79	430	0.11	68	223
15/402	Cuttings	1431–1434	Abu Roash "*A*"	1.00	41.20		0.11	0.79	2.72	429	0.12	79	271
15/403	Cuttings	1440–1443	Abu Roash "*A*"	1.13	37.60		0.13	0.88	2.93	428	0.13	78	260
15/404	Cuttings	1449–1452	Abu Roash "*A*"	1.07	42.35	1.35	0.11	0.74	2.74	428	0.13	69	256
15/405	Cuttings	1458–1461	Abu Roash "*A*"	0.89	46.88		0.11	0.64	2.39	428	0.15	72	269
15/406	Cuttings	1467–1470	Abu Roash "*A*"	0.89	52.25		0.13	0.83	2.81	430	0.14	92	315
15/407	Cuttings	1476–1479	Abu Roash "*A*"	0.89	50.97		0.12	0.77	2.37	430	0.13	86	266
15/408	Cuttings	1485–1488	Abu Roash "*A*"	0.77	71.78	1.06	0.15	0.76	2.28	427	0.17	99	297
15/409	Cuttings	1494–1497	Abu Roash "*A*"	1.22	34.77		0.13	0.82	2.69	424	0.14	67	220
15/410	Cuttings	1503–1506	Abu Roash "*A*"	0.90	45.09		0.12	0.69	1.96	427	0.14	76	218
15/411	Cuttings	1512–1515	Abu Roash "*A*"	0.97	45.36		0.14	0.82	2.18	428	0.15	84	225
15/412	Cuttings	1521–1524	Abu Roash "*A*"	0.88	55.87		0.13	0.70	2.08	429	0.15	80	236
15/413	Cuttings	1530–1533	Abu Roash "*A*"	1.19	42.55		0.13	0.73	2.63	425	0.15	61	220
15/414	Cuttings	1539–1542	Abu Roash "*A*"	1.21	48.71	1.19	0.12	0.81	2.61	426	0.13	67	216
15/415	Cuttings	1548–1551	Abu Roash "*B*"	0.81	66.55	0.86	0.17	1.06	1.85	432	0.13	131	228
15/416	Cuttings	1557–1560	Abu Roash "*B*"	0.78	67.38		0.16	0.93	1.94	432	0.15		
15/417	Cuttings	1566–1569	Abu Roash "*B*"	0.78	90.01		0.39	1.62	1.79	430	0.20	209	230
15/418	Cuttings	1575–1578	Abu Roash "*B*"	0.96	78.78	0.66	0.45	2.12	2.19	430	0.18	222	229
15/419	Cuttings	1587–1590	Abu Roash "*B*"	0.78	90.30		0.33	1.48	2.04	431	0.18	189	261
15/420	Cuttings	1593–1596	Abu Roash "*B*"	0.80	92.55	0.36	0.71	2.34	1.94	428	0.23	294	244
15/421	Cuttings	1602–1605	Abu Roash "*B*"	0.85	74.73		0.17	0.91	2.06	430	0.16	107	244
15/422	Cuttings	1611–1614	Abu Roash "*B*"	1.06	81.21	0.94	0.20	1.25	2.35	433	0.14	118	222
15/423	Cuttings	1620–1623	Abu Roash "*B*"	0.79	73.70		0.14	0.90	2.42	431	0.14	114	306
15/424	Cuttings	1629–1632	Abu Roash "*B*"	0.78	87.08		0.22	0.95	2.53	430	0.19	121	324
15/425	Cuttings	1638–1641	Abu Roash "*C*"	1.01	50.31		0.13	0.80	2.28	430	0.14	79	226
15/426	Cuttings	1647–1650	Abu Roash "*C*"	1.36	29.53	1.52	0.15	0.89	2.92	428	0.14	66	214
15/427	Cuttings	1656–1659	Abu Roash "*C*"	1.24	23.69	1.54	0.13	0.86	2.81	427	0.14	69	226
15/483	Core	1670	Abu Roash "*C*"	0.37	12.39	0.73	0.45	0.64	0.45		0.41		
15/484	Core	1671	Abu Roash "*C*"	0.27	1.47		0.11	0.34	0.40	426	0.23	129	149
15/428	Cuttings	1674–1675	Abu Roash "*C*"	1.20	21.62		0.15	0.79	2.50	427	0.16	65	208
15/486	Core	1678	Abu Roash "*C*"	0.73	0.69		0.21	0.81	0.22	426	0.21	111	31
15/429	Cuttings	1692–1695	Abu Roash "*C*"	1.75	22.71		0.12	0.87	2.51	428	0.13	50	144
15/430	Cuttings	1701–1704	Abu Roash "*D*"	0.96	68.63		0.16	0.87	2.00	433	0.15	91	209

(continued)

Table 2 (continued)

Sample no.	Sample type	Depth (m)	Formation	TOC (%)	CaCO3 (%) ^	TS (%)	*S*1*	*S*2 *	*S*3**	T_{max}***	PI	HI ****	OI *****
15/431	Cuttings	1710–1713	Abu Roash "*D*"	1.03	52.81	1.01	0.15	1.04	2.05	433	0.13	101	199
15/432	Cuttings	1719–1722	Abu Roash "*D*"	0.79	59.33		0.13	0.76	1.95	431	0.15	95	246
15/433	Cuttings	1728–1731	Abu Roash "*D*"	0.89	52.16		0.12	0.72	1.81	432	0.14	81	202
15/434	Cuttings	1737–1740	Abu Roash "*D*"	0.99	56.51		0.10	0.80	1.95	433	0.12	80	196
15/435	Cuttings	1746–1749	Abu Roash "*D*"	0.77	60.39		0.12	0.92	1.95	433	0.12	120	254
15/436	Cuttings	1755–1758	Abu Roash "*D*"	0.74	77.47		0.16	0.94	1.69	434	0.15	127	228
15/437	Cuttings	1764–1767	Abu Roash "*D*"	0.90	63.49		0.14	0.93	1.90	433	0.13	103	212
15/487	Core	1771	Abu Roash "*D*"	0.53	1.12	0.06	0.27	0.88	0.35	433	0.24	167	66
15/488	Core	1772	Abu Roash "*D*"	0.32	96.08		0.12	0.38	0.63	433	0.24	119	198
15/438	Cuttings	1773–1774	Abu Roash "*D*"	1.21	34.73	1.31	0.15	1.03	1.79	431	0.13	85	148
15/490	Core	1777	Abu Roash "*D*"	0.32	112.00		0.15	0.50	0.26	432	0.23	157	81
15/491	Core	1781	Abu Roash "*D*"	1.37	110.50		5.94	12.18	0.44		0.33	887	32
15/439	Cuttings	1782–1783	Abu Roash "*D*"	1.70	20.26		0.09	0.84	1.95	432	0.10	49	114
15/492	Core	1785	Abu Roash "*D*"	1.19	113.99		5.82	5.24	0.33		0.53	442	28
15/493	Core	1787	Abu Roash "*D*"	1.57	110.31		5.82	7.03	0.62		0.45	447	39
15/440	Cuttings	1803–1806	Abu Roash "*D*"	0.88	39.49		0.09	1.02	2.26	436	0.08	116	255
15/441	Cuttings	1812–1815	Abu Roash "*D*"	1.06	54.12		0.13	1.21	2.20	433	0.09	115	208
15/442	Cuttings	1821–1824	Abu Roash "*E*"	1.26	39.23		0.11	1.07	2.36	434	0.09	85	187
15/443	Cuttings	1830–1833	Abu Roash "*E*"	1.41	27.32	1.75	0.12	1.03	2.81	431	0.11	73	199
15/444	Cuttings	1839–1842	Abu Roash "*E*"	1.39	14.94		0.09	0.83	2.85	433	0.09	60	205
15/445	Cuttings	1848–1851	Abu Roash "*E*"	1.32	5.74	0.96	0.10	0.91	2.46	435	0.10	69	186
15/446	Cuttings	1857–1860	Abu Roash "*E*"	1.25	27.55		0.12	0.89	2.13	434	0.12	71	170
15/447	Cuttings	1866–1869	Abu Roash "*E*"	1.06	25.35		0.09	0.66	2.56	432	0.11	62	242
15/448	Cuttings	1875–1878	Abu Roash "*E*"	1.30	16.24	1.04	0.10	0.79	2.34	434	0.11	60	179
15/449	Cuttings	1884–1887	Abu Roash "*E*"	1.17	29.91		0.11	0.76	1.84	432	0.13	64	157
15/450	Cuttings	1902–1905	Abu Roash "*E*"	1.08	32.84	0.87	0.09	0.63	2.13	431	0.12	59	197
15/451	Cuttings	1911–1914	Abu Roash "*E*"	1.40	11.35	1.34	0.11	0.82	2.90	428	0.12	59	207
15/452	Cuttings	1920–1923	Abu Roash "*E*"	1.46	4.09	1.20	0.17	0.89	2.07	428	0.16	61	142
14/1345	Cuttings	1929–1932	Abu Roash "*E*"	1.45	6.67		0.13	0.91	2.16	428	0.13	63	149
15/453	Cuttings	1938–1941	Abu Roash "*E*"	1.54	5.14	1.82	0.11	0.77	2.31	427	0.12	50	150
14/1344	Cuttings	1947–1950	Abu Roash "*E*"	1.55	9.38	1.65	0.13	1.12	2.44	428	0.10	72	157
15/454	Cuttings	1956–1959	Abu Roash "*E*"	1.84	18.62	1.44	0.11	0.96	2.27	431	0.10	52	123
15/455	Cuttings	1965–1968	Abu Roash "*F*"	1.79	30.66	1.26	0.21	2.83	2.27	430	0.07	158	127
15/495	Core	1974	Abu Roash "*F*"	4.00	100.87	0.27	2.43	26.21	1.53	424	0.08	655	38

(continued)

Table 2 (continued)

Sample no.	Sample type	Depth (m)	Formation	TOC (%)	CaCO3 (%) ^	TS (%)	*S1**	*S2* *	*S3***	T_{max}***	PI	HI ****	OI *****
15/456	Cuttings	1974–1975	Abu Roash "*F*"	2.82	46.01	1.05	0.36	7.12	2.30	427	0.05	252	81
15/496	Core	1976	Abu Roash "*F*"	0.32	2.22	0.54	0.10	0.40	0.34	425		127	109
15/497	Core	1977	Abu Roash "*F*"	6.63	55.87	0.32	0.08	0.33	3.40				
15/498	Core	1978	Abu Roash "*F*"	5.87	91.80	1.69	3.11	40.33	1.48	423	0.07	687	25
15/499	Core	1979	Abu Roash "*F*"	4.37	102.82	0.40	2.41	27.13	1.98	421	0.08	621	45
15/457	Cuttings	1983–1986	Abu Roash "*F*"	3.75	57.65	0.93	1.03	14.33	2.59	421	0.07	382	69
15/458	Cuttings	1995–1998	Abu Roash "*G*"	1.91	27.00	1.62	0.15	2.25	2.56	428	0.06	118	134
15/459	Cuttings	2004–2007	Abu Roash "*G*"	1.81	9.55	1.14	0.15	1.87	2.91	431	0.08	103	160
15/460	Cuttings	2015–2018	Abu Roash "*G*"	1.23	8.20		0.12	0.82	1.89	429	0.13	66	154
15/461	Cuttings	2023–2026	Abu Roash "*G*"	1.97	9.16	1.38	0.18	1.72	2.71	432	0.09	87	138
15/462	Cuttings	2043–2047	Abu Roash "*G*"	1.38	3.21	1.04	0.09	0.89	3.03	430	0.09	65	221
15/463	Cuttings	2061–2063	Abu Roash "*G*"	1.35	14.21		0.11	0.90	3.10	432	0.11	67	231
15/464	Cuttings	2070–2073	Abu Roash "*G*"	1.34	28.82		0.36	0.94	2.65	432	0.27	71	199
15/465	Cuttings	2079–2082	Abu Roash "*G*"	1.07	30.22		0.10	0.83	2.67	432	0.11	78	250
15/466	Cuttings	2088–2091	Abu Roash "*G*"	1.43	9.88	1.29	0.11	0.88	2.70	429	0.11	61	190
15/467	Cuttings	2097–2100	Abu Roash "*G*"	1.24	19.62		0.10	0.91	2.60	429	0.10	73	210
15/468	Cuttings	2106–2109	Abu Roash "*G*"	1.24	26.43		0.11	0.83	2.53	430	0.11	67	205
15/469	Cuttings	2115–2118	Abu Roash "*G*"	1.28	27.60		0.14	0.85	2.25	430	0.14	66	176
15/470	Cuttings	2124–2127	Abu Roash "*G*"	1.22	10.95	1.38	0.23	1.99	2.57	432	0.11	164	212
15/471	Cuttings	2133–2136	Abu Roash "*G*"	1.29	17.07		0.08	0.63	2.34	430	0.11	49	182
15/472	Cuttings	2142–2145	Baharyia	1.63	15.42		0.25	1.38	2.94	431	0.15	85	180
15/473	Cuttings	2151–2154	Baharyia	1.65	9.86	1.12	0.19	1.32	3.14	431	0.13	80	190
15/474	Cuttings	2169–2172	Baharyia	1.35	13.74		0.10	0.82	1.91	428	0.11	61	141
15/475	Cuttings	2178–2181	Baharyia	1.30	8.06	1.32	0.08	0.80	2.18	429	0.10	61	167
15/476	Cuttings	2187–2190	Baharyia	1.18	6.17		0.08	0.89	1.56	436	0.08	75	132
15/477	Cuttings	2196–2199	Baharyia	1.95	1.56	0.95	0.23	1.84	2.20	435	0.11	94	113
15/478	Cuttings	2205–2208	Baharyia	1.50	1.66		0.17	1.30	1.85	436	0.12	86	123
15/479	Cuttings	2214–2217	Baharyia	1.56	2.69		0.16	1.50	2.61	434	0.09	96	168
15/480	Cuttings	2223–2226	Baharyia	1.22	15.13	1.33	0.16	1.40	2.35	436	0.10	115	193
15/481	Cuttings	2232–2235	Baharyia	1.54	10.42		0.11	1.02	2.30	434	0.10	66	149
15/482	Cuttings	2235–2238	Baharyia	1.42	35.27	1.18	0.14	0.99	1.72	434	0.12	70	121

^ calcualted from total inorganic carbon
* (mg HC/g rock)
** (mg CO2/g rock)
*** (°C)
**** (mgHC/gTOC)
***** (mgCO2/gTOC)

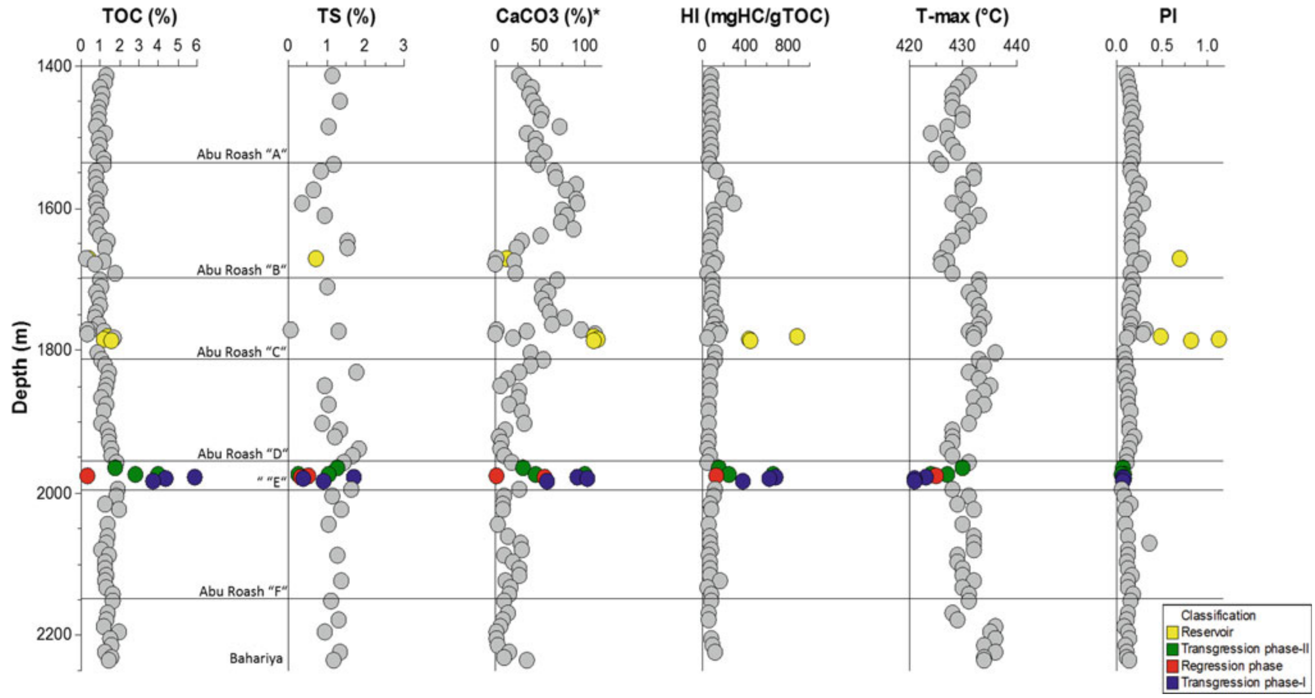

Fig. 5 Total organic carbon (TOC), $CaCO_3$, total sulfur (TS), and rock-eval data versus depth, Bahariya, and Abu Roash formations within the GPT-3 well, Abu Gharadig basin (Ghassal et al., 2018)

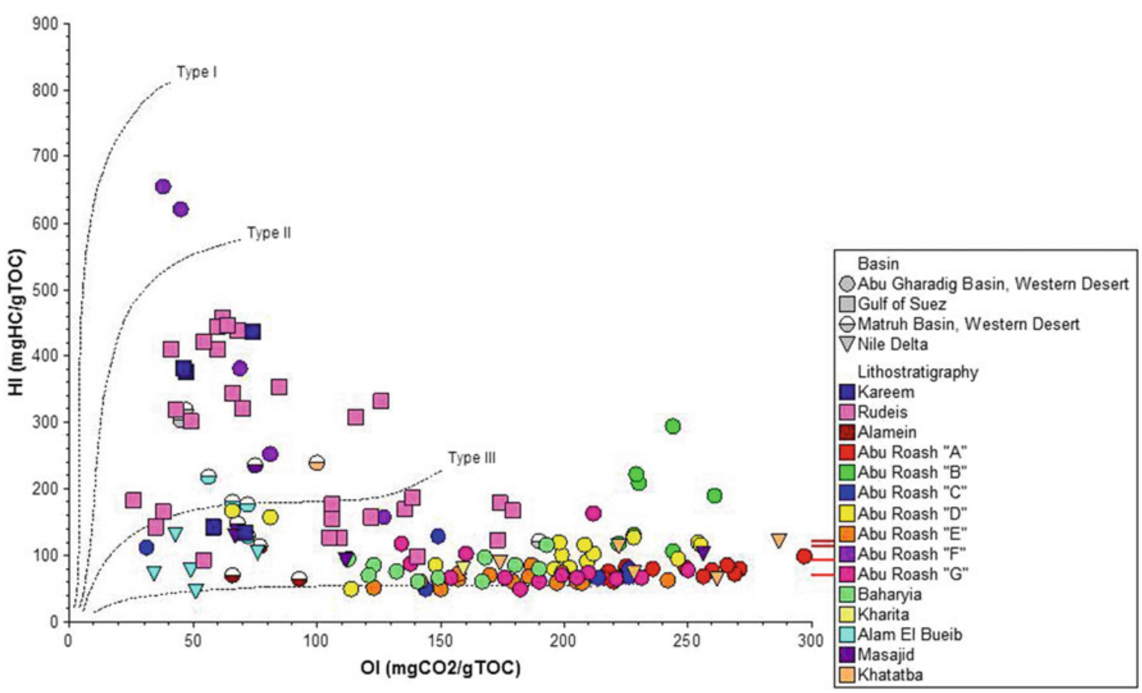

Fig. 6 Pseudo van Krevelen diagram covers most of the known source rock intervals within different basins in Egypt. Data are available in Tables 1, 2, 3, 4 and 5

nature of the source rocks for the Abu Hammad-1 well as follows:

1. Highly oil-prone and mature source rocks with amorphous organic matter in the lower Masajid, Khatatba, and middle Rajabiah formations.

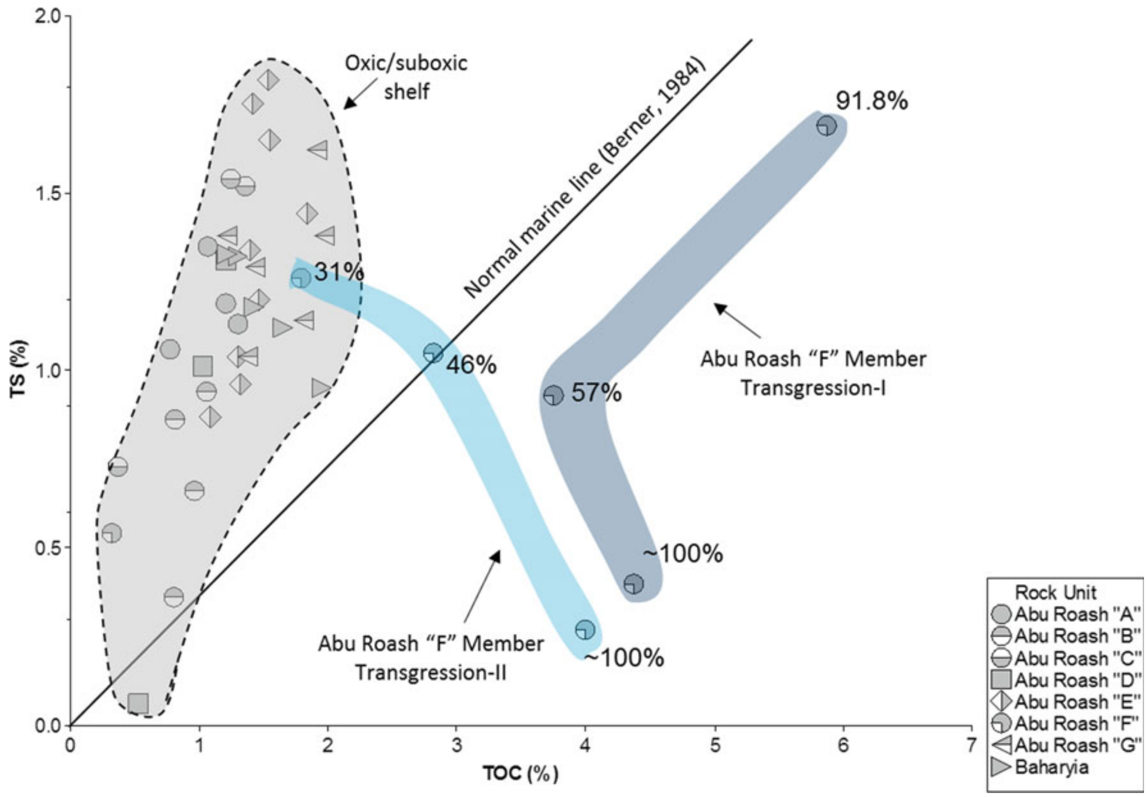

Fig. 7 TS versus TOC showing the characteristic signature of the Abu Roash "*F*" Member. The samples are classified into three groups, which are: (1) Abu Roash "*F*" Member transgression-1; (2) Abu Roash "*F*" member transgression-2; and (3) oxic/suboxic shelf: the samples from the rest of the rock units. $CaCO_3$ was calculated from total inorganic carbon (Ghassal et al., 2018)

2. Highly oil-prone but immature source rocks with amorphous organic matter in the Alamein and Alam El Bueib formations.
3. Oil-prone, mature source rocks in the upper Masajid Formation.
4. Gas-prone, mature source rocks in the upper Rajabiah Formation.

However, geochemical investigation of the Abu Hammad-1 well by Ghassal et al. (2016) suggests that the Upper Jurassic Masajid and the Lower Cretaceous Alam El Bueib formations contain gas-prone source rock, with TOC up to 4.0 wt.% and HI ranging from 46 to 130 mg HC/g TOC (Table 3). Microscopic investigation reveals that these source rocks are dominated by vitrinite, inertinite, and coaly particles (Fig. 10). Furthermore, T_{max} and vitrinite reference (VRe) indicate low thermal maturity.

4.3 Cenozoic Source Rocks

Palynological studies dealing with the Cenozoic of Egypt are somewhat dispersed and few in comparison with those carried out on older strata. Moreover, among the relatively limited number of publications, palynofacies studies targeting are even fewer. These studies are available only from the Gulf of Suez and the Nile Delta, and there is one case from the north Western Desert.

4.3.1 North Western Desert

From a palynofacies perspective, El Beialy et al. (2016) introduced the first study that dealt with the kerogen portion of the subsurface material (Amana-1X well) within the Dabaa Formation. They utilized palynofacies analysis to study the hydrocarbon potential of the organic matter and provided a comprehensive interpretation of the prevailing paleoenvironmental conditions (Fig. 11). As a result, they established two major marine palynofacies. The older palynofacies (palynofacies 1) contained Type II/III kerogen (mostly oil-prone), which was formed in an outer shelf to upper slope under suboxic to anoxic settings. Palynofacies 2 comprised Type III kerogen (largely gas-prone) that signifies shallower, more terrestrially influenced circumstances. However, SCI determination (spore coloration measurements) implied thermally mature conditions for both palynofacies. There was no verification by organic geochemistry.

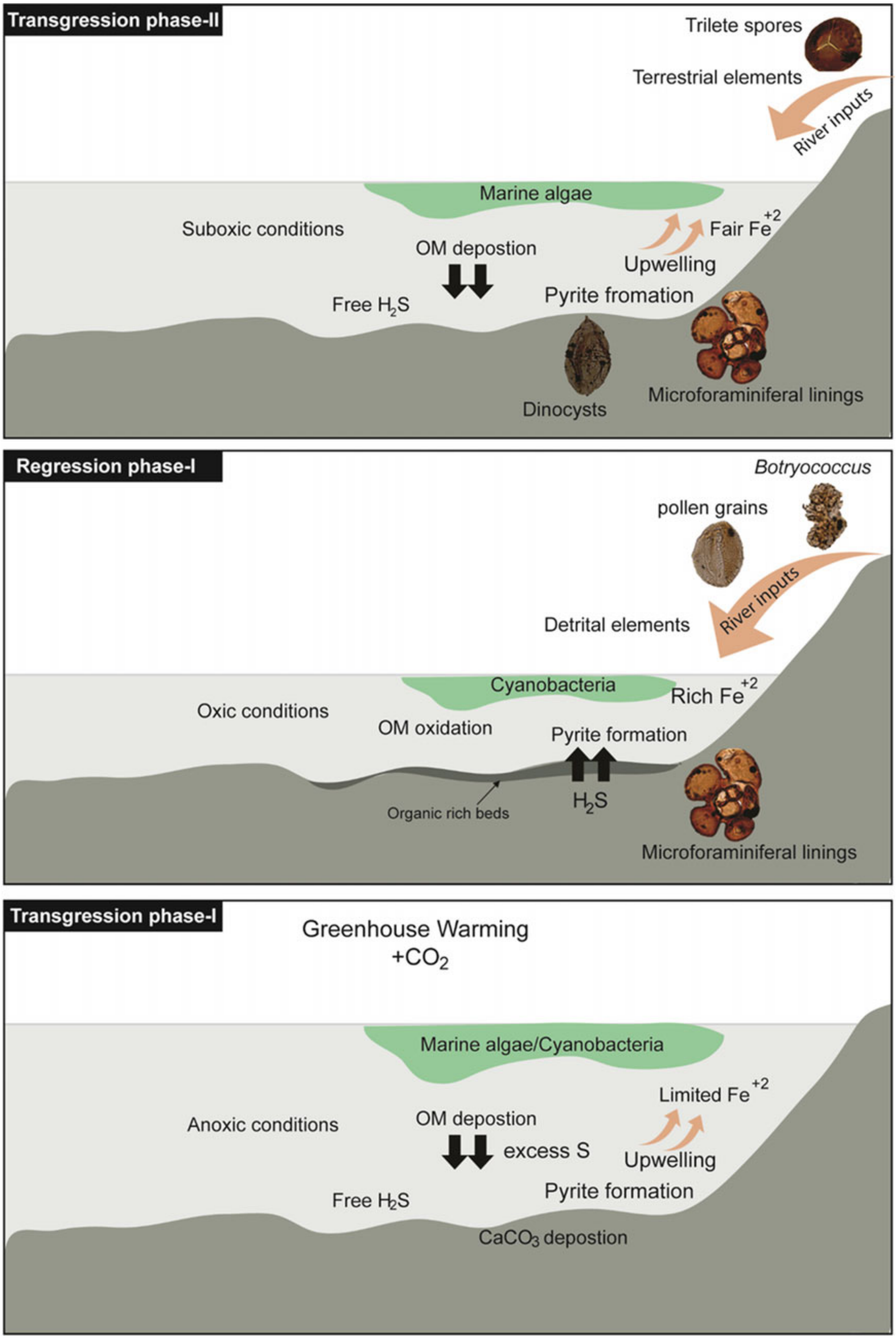

Fig. 8 Comprehensive depositional model of the Abu Roash "*F*" member, depended on an integrated geochemical and palynological interpretation of the Abu Gharadig Basin (Ghassal et al., 2018)

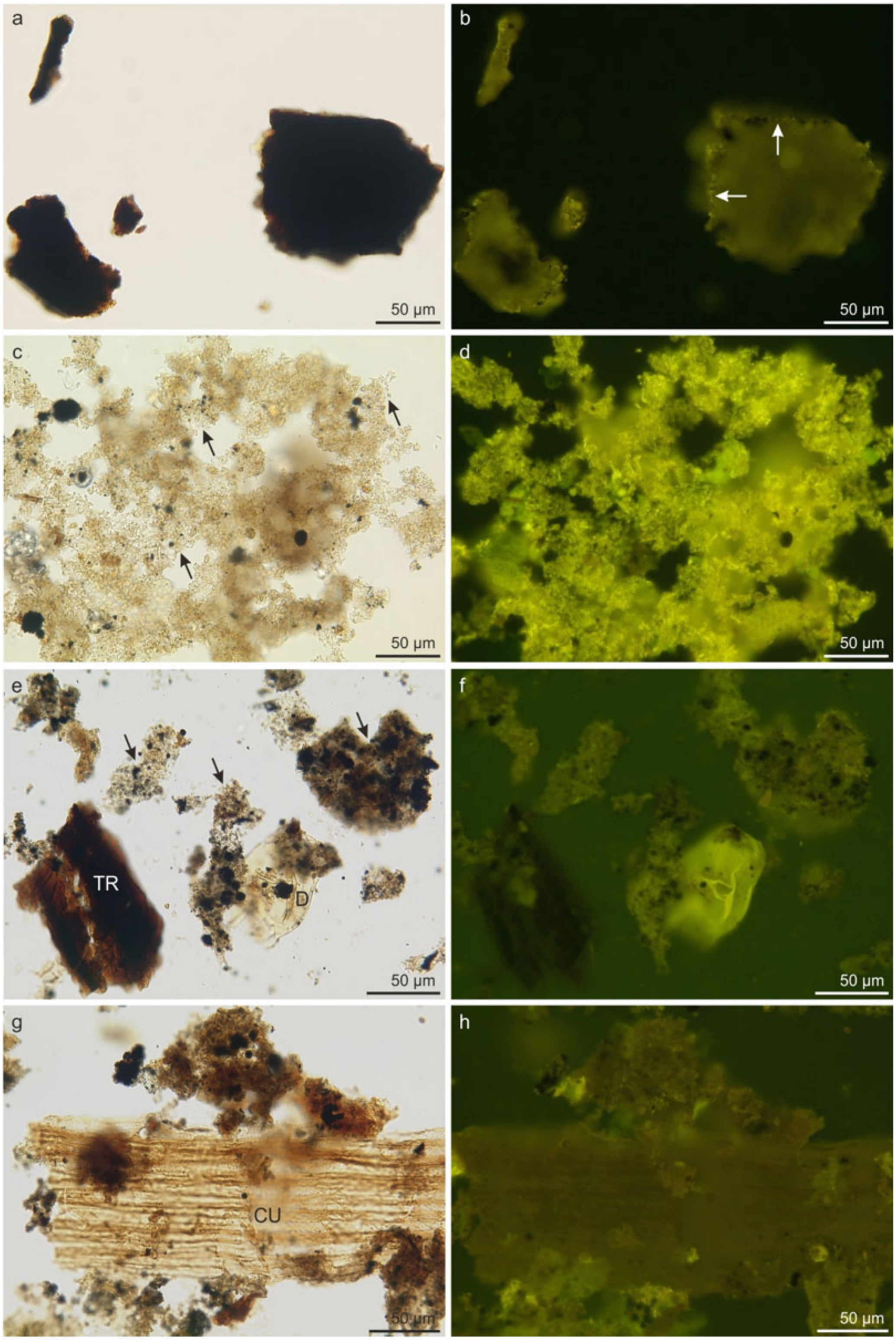

Fig. 9 Palynofacies assemblages from the central Gulf of Suez, Egypt (reproduced from El Diasty et al., 2014). **a** Non-marine AOM flakes may characterize amorphous biodegraded phytoclasts (Thebes Formation); **b** fluorescent AOM aggregates, a distinctly structured rim (arrows) might signify biodegradation or transformation of phytoclasts into AOM (Thebes Formation). **c** Fine granular, yellow to gray (arrows) marine amorphous masses, apparently of algal origin (Thebes Formation); **d** highly fluorescent AOM, may reflect an algal origin (Thebes formation). **e** A mixed palynofacies association comprised mainly AOM (arrows) with dispersed pyrites, tracheid phytoclast (TR) and dinoflagellate cyst (D) may represent *Isabelidinium*/*Chatangiella* sp. (Matulla Formation); **f** a variable fluorescent potential among the different palynofacies components (Matulla formation); **g** a dispersed leaf cuticle (CU) phytoclast displays a regular, rectangular cellular structure bounded by AOM (Matulla formation); **h** a dispersed leaf cuticle shows very weak fluorescence (Matulla formation)

Table 3 TOC, rock-eval, elemental data, and vitrinite reflectance equivalent (VRe) of the upper Jurassic Masajid and the lower Cretaceous Alam El Bueib formations (Abu Hammad-1 well), Nile Delta, Egypt (Ghassal et al., 2016)

Sample number	Well name	Depth (m)	Formation	Age	TOC (wt.%)	TIC (%)	$CaCO_3$ (%)	TS (%)	TOC/TS	S_1	S_2	S_3	Tmax °C	HI	OI	VR (%)
15/215	Abu Hammad-1	1212	Kharita	U. Cretaceous	0.36	11.56	96.34	0.78	0.47	0.09	0.26	1.21	428	70	331	
15/216		1242	Kharita	U. Cretaceous	0.79	3.02	25.15	0.70	1.13	0.11	0.63	1.25	421	80	159	
15/217		1362	Kharita	U. Cretaceous	0.58	10.95	91.28	0.99	0.59	0.24	0.36	1.09				
15/218		1461	Alam El-Bueib	L. Cretaceous	1.67	1.94	16.18			0.67	1.74	1.26	427	104	76	
14/1350		1605	Alam El-Bueib	L. Cretaceous	3.56	0.51	4.23	2.11	1.69	0.49	4.62	1.54	422	130	43	0.42
14/1351		1794	Alam El-Bueib	L. Cretaceous	3.46	0.23	1.96	1.26	2.74	0.25	2.65	1.69	426	77	49	
15/221		1803	Alam El-Bueib	L. Cretaceous	3.88	0.31	2.62	0.98	3.96	0.52	2.78	1.32	429	72	34	
15/222		1947	Alam El-Bueib	L. Cretaceous	3.18	0.22	1.85	2.23	1.43	0.38	1.45	1.64	423	46	51	0.47
15/223		1965	Masajid	U. Jurassic	1.74	3.14	26.17	1.18	1.47	2.44	2.22	1.17	428	128	67	
15/224		2016	Masajid	U. Jurassic	1.18	1.26	10.46	1.35	0.87	0.29	1.10	1.32	427	93	112	
14/1352		2034	Masajid	U. Jurassic	0.58	4.78	39.80	1.20	0.48	0.07	0.59	1.48	422	102	256	
15/226		2379	Khatatba	M. Jurassic	0.63	7.44	61.98			0.20	0.71	1.39	432	113	222	
15/227		2448	Khatatba	M. Jurassic	0.66	6.13	51.06	0.92	0.71	0.09	0.58	1.14	429	89	174	
14/1353		2502	Khatatba	M. Jurassic	0.53	3.02	25.14	0.82	0.65	0.07	0.65	1.53	426	121	287	0.63
15/229		3306	Khatatba	M. Jurassic	0.57	3.99	33.25	0.84	0.68	0.05	0.41	1.29	434	73	228	
15/230		3537	Khatatba	M. Jurassic	0.51	5.27	43.93			0.04	0.33	1.33	433	64	262	0.71

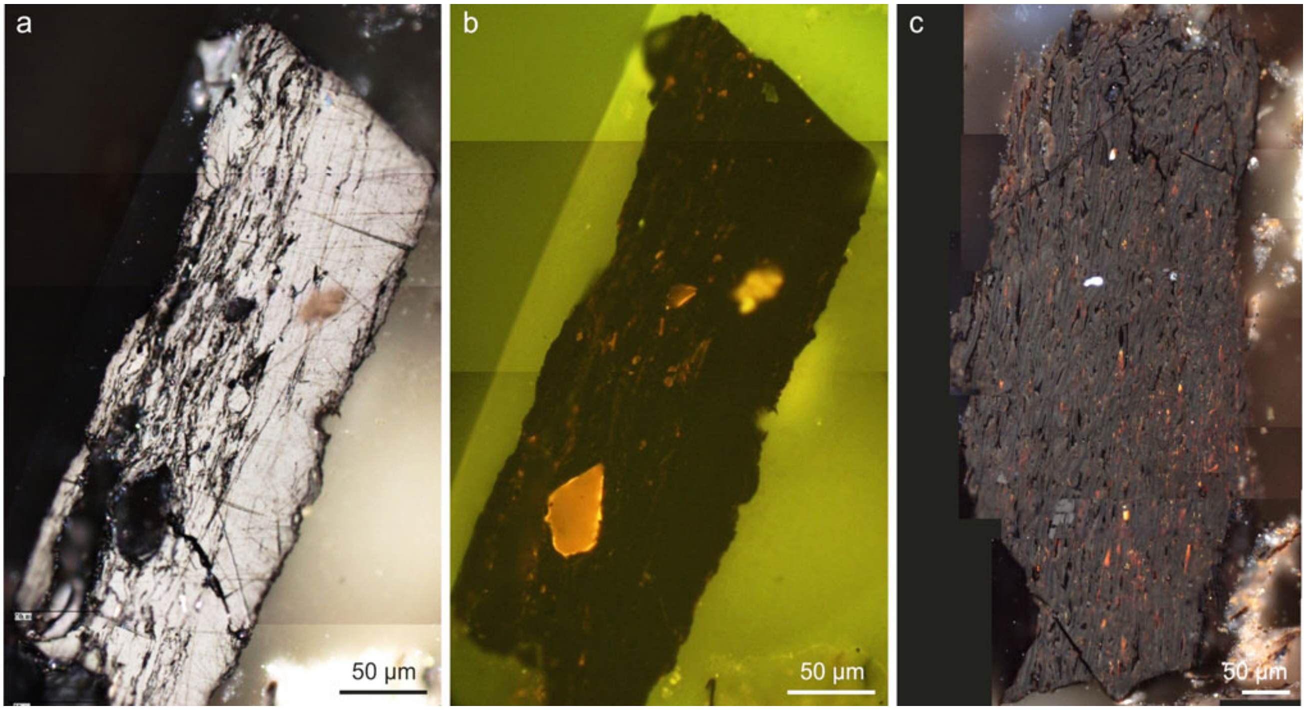

Fig. 10 Organic microscopy photographs from the Nile Delta source rock. **a b** Allochthonous coal particles under incident and fluorescent lights; **c** tellovitrinite under incident light

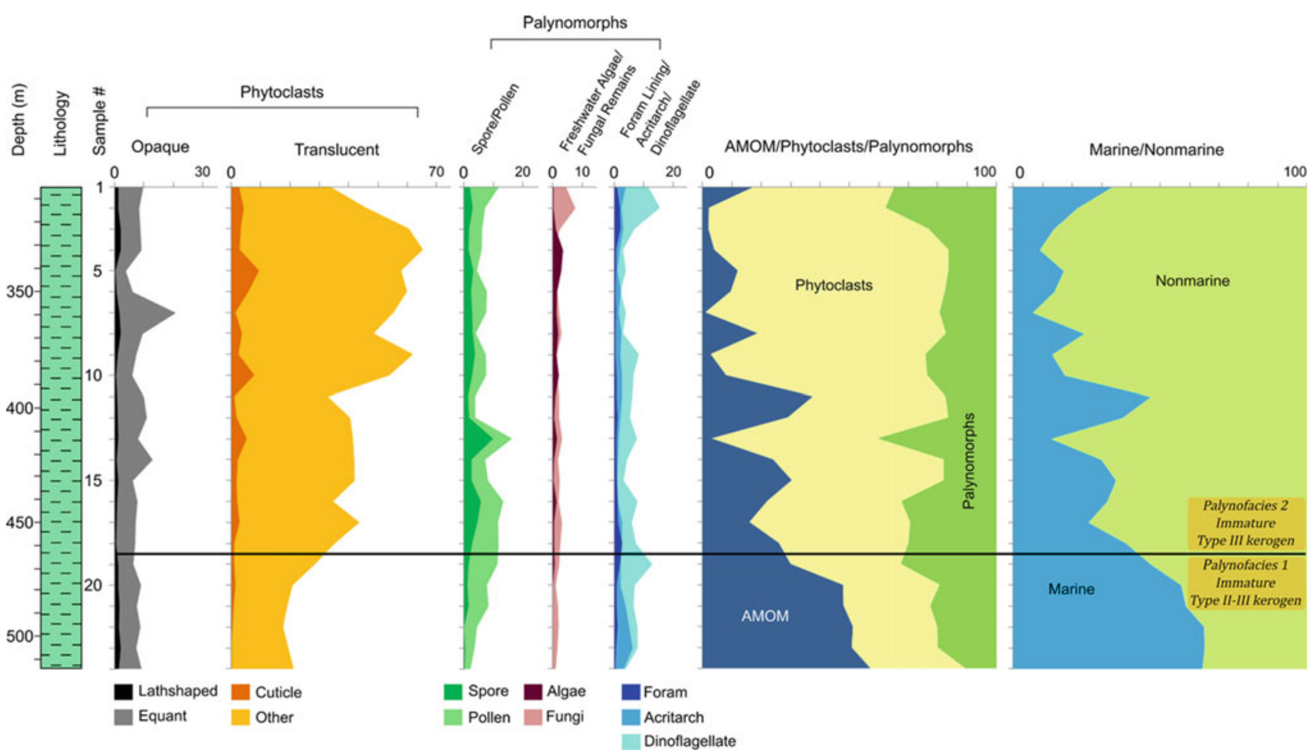

Fig. 11 Quantitative distribution of the different kerogen components of the Oligocene Dabaa Formation, AMOM represents amorphous marine organic matter (El Beialy et al., 2016)

Table 4 TOC and rock-eval pyrolysis results of the Miocene samples (GH 404-2A, GH 420-1, and SA-E6A wells), Gulf of Suez, Egypt (El Atfy et al., 2014)

Rock eval 6 data

Well name	Sample	Status	Depth [m]	Formation	TOC [wt.%]	S_1 [mg HC/Rock]	S_2 [mg HC/Rock]	S_3 [mg CO2/Rock]	T_{max} [°C]	PI $S1/(S1 + S2)$	HI $S2*100/TOC$	OI $S3*100/TOC$	S_2/S_3
SA-E6A	SA_013	Extracted	1405.1	Kareem	2.27		8.50	1.07	419		375	47	7.93
SA-E6A		Non-extracted			8.75		10.43	0.96	426				
SA-E6A	SA_015	Extracted	1466.1	Rudeis	2.69		11.01	1.62	425		410	60	6.81
SA-E6A		Non-extracted			8.96		16.03	1.27	420				
GH 404-2A	04_072	Non-extracted	2542.0	Kareem	2.26	0.99	3.03	1.60	432	0.25	134	71	1.90
GH 404-2A	04_076	Non-extracted	2578.6	Kareem	1.40	0.39	1.99	0.81	436	0.17	142	58	2.44
GH 404-2A	04_082	Non-extracted	2633.5	Rudeis	1.33	0.62	1.64	2.30	437	0.28	123	173	0.71
GH 404-2A	04_086	Non-extracted	2670.0	Rudeis	2.04	1.80	6.78	2.57	434	0.21	332	126	2.63
GH 404-2A	04_090	Non-extracted	2706.6	Rudeis	2.24	0.41	2.83	2.45	438	0.13	127	109	1.16
GH 404-2A	04_094	Non-extracted	2743.2	Rudeis	2.40	0.78	3.72	2.56	439	0.17	155	106	1.46
GH 404-2A	04_098	Non-extracted	2779.8	Rudeis	2.35	0.69	3.33	0.82	437	0.17	142	35	4.04
GH 404-2A	04_102	Non-extracted	2816.4	Rudeis	1.97	0.32	1.83	1.06	437	0.15	93	54	1.72
GH 404-2A	04_110	Non-extracted	2889.5	Rudeis	1.28	0.55	1.62	1.34	437	0.25	127	105	1.21
GH 404-2A	04_118	Non-extracted	2962.7	Rudeis	1.40	0.82	2.50	2.43	437	0.25	179	174	1.03
GH 404-2A	04_122	Non-extracted	2999.2	Rudeis	2.32	1.75	4.23	0.61	436	0.29	182	26	6.95
GH 404-2A	04_126	Non-extracted	3045.0	Rudeis	1.68	2.68	5.18	1.95	439	0.34	308	116	2.66
GH 404-2A	04_130	Non-extracted	3081.5	Rudeis	1.21	0.77	2.02	2.16	439	0.28	167	179	0.93
GH 404-2A	04_134	Non-extracted	3118.1	Rudeis	2.60	0.93	2.57	3.67	439	0.27	99	141	0.70
GH 404-2A	04_140	Non-extracted	3173.0	Rudeis	1.88	1.31	3.17	2.56	439	0.29	169	136	1.24
GH 404-2A	04_142	Non-extracted	3191.3	Rudeis	1.50	3.33	2.36	1.84	441	0.59	157	122	1.29
GH 404-2A	04_144	Non-extracted	3209.5	Rudeis	1.90	0.96	3.34	2.00	439	0.22	176	106	1.67
GH 404-2A	04_146	Non-extracted	3227.8	Rudeis	1.76	2.22	3.28	2.44	442	0.40	186	139	1.34
GH 404-2A	04_150	Non-extracted	3264.4	Rudeis	1.69	1.40	2.80	0.64	442	0.33	165	38	4.37
GH 420-1	20_048	Extracted	2200.7	Kareem	3.17		12.06	1.46	421		381	46	8.27
		Contaminated			7.16		12.82	1.70	428				
GH 420-1	20_049	Extracted	2231.1	Kareem	2.18		9.50	1.60	422		436	74	5.93
		Contaminated			6.49		9.45	1.42	432				
GH 420-1	20_052	Extracted	2258.6	Rudeis	2.45		11.21	1.51	423		458	62	7.43
		Contaminated			7.15		9.62	1.35	439				
GH 420-1	20_055	Extracted	2286.0	Rudeis	1.81		5.81	1.26	421		321	70	4.60
		Contaminated			7.62		15.11	1.34					

(continued)

Table 4 (continued)

Rock eval 6 data													
Well name	Sample	Status	Depth [m]	Formation	TOC [wt.%]	S_1 [mg HC/Rock]	S_2 [mg HC/Rock]	S_3 [mg CO2/Rock]	T_{max} [°C]	PI $S1/(S1 + S2)$	HI $S2$*100/TOC	OI $S3$*100/TOC	S_2/S_3
GH 420-1	20_059	Extracted	2322.6	Rudeis	2.26		9.88	1.53	424		438	68	6.46
		Contaminated			7.29		10.52	1.46					
GH 420-1	20_063	Extracted	2359.2	Rudeis	3.36		10.15	1.66	433		302	49	6.10
		Contaminated			7.59		12.57	1.54					
GH 420-1	20_069	Extracted	2414.0	Rudeis	2.72		12.13	1.63	426		445	60	7.45
		Contaminated			8.43		11.04	1.42	432				
GH 420-1	20_075	Extracted	2468.9	Rudeis	2.82		11.87	1.53	421		421	54	7.76
		Contaminated			7.62		9.71	1.60	432				
GH 420-1	20_077	Extracted	2487.2	Rudeis	3.42		13.96	1.39	425		409	41	10.04
		Contaminated			9.37		12.43	0.45					
GH 420-1	20_081	Extracted	2523.7	Rudeis	3.20		10.17	1.39	426		318	43	7.33
		Contaminated			9.97		11.69	0.44					
GH 420-1	20_084	Extracted	2551.2	Rudeis	1.89		8.42	1.21	429		446	64	6.97
		Contaminated			8.95		15.94	1.49					
GH 420-1	20_090	Extracted	2606.0	Rudeis	1.58		5.59	1.34	428		353	85	4.17
		Contaminated			8.71		1.28	0.04	418				
GH 420-1	20_093	Extracted	2633.472	Rudeis	2.59		8.90	1.72	427		343	66	5.17
		Contaminated			7.06		10.31	1.83	429				

Table 5 TOC, rock-eval, elemental data, and VRe of Miocene and Pliocene rock units (Matariya-1 well), Nile Delta, Egypt (Ghassal et al., 2016)

Sample number	Well name	Depth (m)	Formation	Age	TOC (wt.%)	TIC (%)	$CaCO_3$ (%)	TS (%)	TOC/TS	S_1	S_2	S_3	T_{max} °C	HI	OI	VR (%)
15/190	Matariya-1	2284	Kafr El Sheikh	M. Pliocene	0.51	0.42	3.49			0.06	0.30	1.21				
15/191	Matariya-1	2311	Kafr El Sheikh	M. Pliocene	0.29	0.53	4.42			0.07	0.27	1.15				
15/192	Matariya-1	2368	Qawasim	U. Miocene	0.57	0.37	3.09			0.06	0.36	1.28	416	63	225	
15/193	Matariya-1	2479	Qawasim	U. Miocene	0.59	0.41	3.42			0.06	0.37	1.27	424	64	215	
15/194	Matariya-1	2503	Qawasim	U. Miocene	0.50	0.24	2.01			0.04	0.33	1.29	412	65	258	0.48
15/195	Matariya-1	2590	Qawasim	U. Miocene	0.59	0.28	2.33			0.07	0.39	1.15	428	66	196	
15/196	Matariya-1	2629	Qawasim	U. Miocene	0.71	0.33	2.73	1.09	0.66	0.10	0.60	1.27	415	84	178	
15/197	Matariya-1	2659	Qawasim	U. Miocene	0.51	0.22	1.86			0.05	0.33	1.30	425	64	257	
15/198	Matariya-1	3113	Qawasim	U. Miocene	1.28	1.11	9.28	0.98	1.31	0.15	0.89	1.30	428	69	101	
15/199	Matariya-1	3293	Qawasim	U. Miocene	1.30	0.23	1.92			0.13	0.83	1.13	428	64	87	
15/200	Matariya-1	3362	Sidi Salem	M. Miocene	1.06	0.35	2.93	0.86	1.24	0.07	0.55	1.28	434	52	120	
14/1354	Matariya-1	3380	Sidi Salem	M. Miocene	0.99	0.26	2.16	0.90	1.10	0.06	0.59	1.45	426	60	146	
15/202	Matariya-1	3443	Sidi Salem	M. Miocene	1.03	0.28	2.32			0.15	0.63	1.22	428	61	119	
15/203	Matariya-1	3482	Sidi Salem	M. Miocene	1.35	0.36	3.03	0.80	1.68	0.12	1.04	1.13	426	77	84	
15/204	Matariya-1	3527	Sidi Salem	M. Miocene	1.59	0.42	3.48	0.96	1.66	0.08	0.66	1.27	428	41	80	
15/205	Matariya-1	3560	Sidi Salem	M. Miocene	1.17	0.29	2.38			0.07	0.61	1.28	429	53	109	0.53
15/206	Matariya-1	3593	Sidi Salem	M. Miocene	1.46	0.41	3.45			0.16	1.17	1.27	428	80	87	
14/1355	Matariya-1	3626	Sidi Salem	M. Miocene	1.32	0.64	5.34			0.09	0.84	1.53	425	64	116	
15/208	Matariya-1	3647	Sidi Salem	M. Miocene	2.08	1.23	10.25	1.24	1.68	0.31	1.71	1.50	433	82	72	
15/209	Matariya-1	3740	Sidi Salem	M. Miocene	2.88	1.14	9.52	1.09	2.65	0.77	3.04	1.38	430	105	48	
15/210	Matariya-1	3824	Sidi Salem	M. Miocene	0.95	0.41	3.39			0.77	1.31	1.44	416	139	152	
15/211	Matariya-1	4002	Sidi Salem	M. Miocene	1.70	0.88	7.32	0.89	1.91	0.95	2.31	1.11				
15/212	Matariya-1	4035	Sidi Salem	M. Miocene	1.11	0.71	5.93	1.10	1.01	0.36	1.29	1.13				
15/213	Matariya-1	4108	Sidi Salem	M. Miocene	1.65	0.76	6.37			0.66	1.76	1.26	420	106	76	
15/214	Matariya-1	4141	Sidi Salem	M. Miocene	1.38	0.62	5.20			0.92	2.52	1.25	423	183	90	0.66

4.3.2 Gulf of Suez

Mainly, the Miocene has been studied in the Gulf of Suez. In spite of the intense micropaleontologic efforts (mainly foraminifera and calcareous nannofossils) in the last years, few contributions have been published on the palynology of this region in comparison with other parts of Egypt. Until recently, there were few palynological studies (mainly biostratigraphic) on the Miocene deposits of the Gharandal and Ras Malaab groups, which are considered among the most important hydrocarbon-bearing sequences in Egypt. Therefore, introducing palynofacies herein especially as a maturation detection parameter covers such a niche.

To the authors' knowledge, El Atfy et al., (2013, 2014) introduced palynofacies research to the Miocene of the Gulf of Suez. These publications integrated palynofacies with organic geochemistry and organic petrography to attain the following results:

1. Palynofacies analyses discriminated the Nukhul Formation into three of two main palynofacies assemblages (PF-Ia, PF-Ib, and PF-II): PF-Ia and PF-Ib were the dominant facies within the Ghara Member, representing a suboxic–anoxic environment. Kerogen Type III was established for these two assemblages. PF-II mainly dominated the Shoab Ali Member, showing a composition of mixed Type III and Type II kerogen with more phytoclast input supporting a fairly continental suboxic–anoxic basin characterized by low AOM. These results were in great accordance with previous organic geochemical analyses (El Atfy et al., 2013).
2. TOC and Rock-Eval analyses suggested a fair to good organic richness for the Rudeis and Kareem formations (Table 4). According to palynofacies analyses and organic petrology, Type III or Type II/III kerogen were identified with a very limited terrestrial input. Furthermost of the sediments were deposited under oxygen-deficient, but not totally anoxic, conditions. Multi-proxy thermal maturation determination techniques indicated an immature to early mature level for the organic matter and a rise of maturation with depth.

4.3.3 Nile Delta

The study carried out by Ibrahim (1996) on core samples retrieved from El Qara-2 borehole in the north-central Nile Delta was the only attempt to employ palynofacies as an exploration proxy within the basin. SCI index enabled him to recognize three organic facies, immature, mature (Kafr El Sheikh Formation), and overmature (Abu Madi Formation).

The Miocene source rocks of the Nile Delta, on the other hand, were studied in more detail by organic geochemistry by Ghassal et al. (2016) who provided a comprehensive review of the regional source characteristics (Table 5). The central Nile Delta Basin possesses higher source rock quality than the eastern part. The difference in quality is ascribed to the variation of the depositional setting. The eastern Nile Delta Basin was deposited in shallower water settings during the Middle Miocene time. For example, the highest reported HI values in the eastern part of the delta is 184 mgHC/gTOC, whereas it reaches 480 mgHC/gTOC in the western part of the basin (El Nady, 2007; El Nady & Harb, 2010; Ghassal et al., 2016; Keshta et al., 2012; Shaaban et al., 2006).

5 Conclusions

The integration of optical and geochemical techniques represents the best way to screen hydrocarbon source rock potential and has a distinguishing impact on kerogen analysis, besides its utilization in paleoenvironmental inferences. It is worth noting that while kerogen types are usually obtained from Rock-Eval data, palynofacies and organic petrographic data offer additional reliable information. For samples with low to moderate TOC, Rock-Eval data are mostly uncertain for the reason that the retained hydrocarbons in the mineral matrix (Grohmann et al., 2018). Consequently, palynofacies analysis is a valuable, complementary technique for investigating the petroleum generation potential of source rocks.

Acknowledgements The authors are also grateful to the Egyptian General Petroleum Corporation (EGPC) and the operating companies for the provision of samples and well logs during the past ten years during which this research was conducted. The first author acknowledges the financial support from the Alexander von Humboldt Foundation, Germany (EGY-1190326-GF-P). Insightful reviews by two anonymous referees enabled an improved presentation of this work.

References

Abohajar, A., Littke, R., Schwarzbauer, J., Weniger, P., & Boote, D. R. D. (2015). Biomarker characteristics of potential source rocks in the Jabal Nafusah area, NW Libya: Petroleum systems significance. *Journal of Petroleum Geology, 38*(2), 119–156.

Abu-Ali, M., & Littke, R. (2005). Paleozoic petroleum systems of Saudi Arabia: a basin modeling approach. *GeoArabia, 10*(3), 131–168.

Bakun, A. (1990). Global climate change and intensification of coastal ocean upwelling. *Science, 247*(4939), 198–201.

Barakat, M. K. A. (2010). Modern geophysical techniques for constructing a 3D geological model on the Nile Delta, Egypt. Dissertation, Technical University of Berlin. https://doi.org/10.14279/depositonce-2627

Bassett, M. G. (2009). Early Palaeozoic peri-Gondwana terranes: New insights from tectonics and biogeography. *Geological Society, London, Special Publications, 325*, 1–2. https://doi.org/10.1144/SP325.1

Batten, D. J. (1982). Palynofacies, palaeoenvironments and petroleum. *Journal of Micropalaeontology, 1*, 107–114.

Batten, D. J. (1996a). Palynofacies and palaeoenvironmental interpretation. In J. Jansonius, D. C. McGregor (Eds.), *Palynology: Principles and applications 3* (pp. 1011–1064). AASP Foundation

Batten, D. J. (1996b). Palynofacies and petroleum potential. In J. Jansonius, D. C. McGregor (Eds.), *Palynology: Principles and applications 3* (pp. 1065–1084). AASP Foundation

Batten, D. J. (1999). Palynofacies analysis. In T. P. Jones & N. P. Rowe (Eds.), *Fossil plants and spores: Modern techniques* (pp. 194–198). Geological Society.

Belaid, A., Krooss, B. K., & Littke, R. (2010). Thermal history and source rock characterization of a Paleozoic section in the Awbari Trough, Murzuq Basin, SW Libya. *Marine and Petroleum Geology, 27*, 612–632.

Berra, F., Angiolini, L. (2014). The evolution of the Tethys Region throughout the Phanerozoic: a brief tectonic reconstruction. In L. Marlow, C. C. G. Kendall, L. A. Yose (Eds.), *Petroleum systems of the Tethyan region* (vol. 106, pp. 1–27). AAPG Memoir

Beydoun, Z. R. (1998). Arabia plate oil and gas: Why so rich and so prolific. *Episodes, 21*(2), 1–8.

Bosworth, W., Huchon, P., & McClay, K. (2005). The Red Sea and Gulf of Aden Basins. *Journal of African Earth Sciences, 43*, 334–378.

Bustin, R. M. (1988). Sedimentology and characteristics of dispersed organic matter in Tertiary Niger Delta: Origin of source rocks in a deltaic environment. *AAPG Bulletin, 72*(3), 277–298.

Coe, A. L., Bosence, D. W. J., Church, K. D., Flint, S. S., Howell, J. A., & Wilson, R. C. L. (2003). *The sedimentary record of sea-level change* (p. 2003). Cambridge University Press and the Open University.

Combaz, A. (1964). Les palynofaciès. *Revue De Micropaléontologie, 7*, 205–218.

Craig, J., Thurow, J., Thusu, B., Whitham, A., & Abutarruma, Y. (2009). Global Neoproterozoic petroleum systems: The emerging potential in North Africa. *Geological Society, London, Special Publications, 326*, 1–25.

Dolson, J., et al. (2020). The petroleum geology of Egypt and history of exploration. In Z. Hamimi (Ed.), *The geology of Egypt* (pp. 635–658). Springer.

Dolson, J. C., Atta, M., Blanchard, D., Sehim, A., Villinski, J., Loutit, T., Romine, K. (2014). Egypt's future petroleum resources: a revised look in the 21st Century. In L. Marlow, C. Kendall, L. Yose (Eds.), *Petroleum systems of the Tethyan region, Memoir* (vol. 106, pp. 143–178). AAPG

Dolson, J. C., Shann, M. V., Matbouly, S. I., Hammouda, H., & Rashed, R. M. (2000). Egypt in the twenty-first century: Petroleum potential in offshore trends. *GeoArabia, 6*(2), 211–230.

Duarte, L. V., Silva, R. L., Mendonça Filho, J. G., Ribeiro, N. P., & Chagas, R. B. A. (2012). High-resolution stratigraphy, palynofacies and source rock potential of the Agua de Madeiros formation (lower Jurassic), Lusitanian basin, Portugal. *Journal of Petroleum Geology, 35*(2), 105–126.

El Atfy, H. (2021). Palynofacies as a paleoenvironment and hydrocarbon source potential assessment tool: An example from the Cretaceous of north Western Desert, Egypt. *Palaeobiodiversity and Palaeoenvironments, 101*, 35–50.

El Atfy, H., Brocke, R., Uhl, D. (2013). Age and paleoenvironment of the Nukhul Formation, Gulf of Suez, Egypt: Insights from palynology, palynofacies and organic geochemistry. *GeoArabia, 18*(4), 137–174

El Atfy, H., Brocke, R., Uhl, D., Ghassal, B., Stock, A. T., Littke, R. (2014). Source rock potential and paleoenvironment of the Miocene Rudeis and Kareem formations, Gulf of Suez, Egypt: An integrated palynofacies and organic geochemical approach. *International Journal of Coal Geology, 131*, 326–343

El Atfy, H., Ghassal, B., Maher, A., Hosny, A., Mostafa, A., & Littke, R. (2019). Palynological and organic geochemical studies of the upper Jurassic-lower cretaceous successions, Western Desert, Egypt: Implications for paleoenvironment and hydrocarbon source rock potential. *International Journal of Coal Geology, 211*, 103207.

El Beialy, S. Y., El Atfy, H. S., Zavada, M., El Khoriby, E. M., & Abu Zied, R. H. (2010). Palynological, palynofacies, paleoenvironmental and organic geochemical studies on the upper cretaceous succession of the GPTSW-7 Well, North Western Desert, Egypt. *Marine and Petroleum Geology, 27*, 370–385.

El Beialy, S. Y., Zobaa, M. K., & Taha, A. A. (2016). Depositional paleoenvironment and hydrocarbon source potential of the Oligocene Dabaa formation, North Western Desert, Egypt: A palynofacies approach. *Geosphere, 12*, 346–353.

El Diasty, W. S., El Beialy, S., Abo Ghonaim, A. A., Mostafa, A. R., & El Atfy, H. (2014). Palynology, palynofacies and petroleum potential of the upper cretaceous-Eocene Matulla, brown limestone and thebes formations, Belayim oilfields, central Gulf of Suez, Eqypt. *Journal of African Earth Sciences, 95*, 155–167.

El Nady, M. M. (2007). Organic geochemistry of source rocks, condensates, and thermal geochemical modeling of Miocene sequence of some wells, onshore Nile Delta, Egypt. *Petroleum Science and Technology, 25*, 791–817.

El Nady, M. M., & Harb, F. M. (2010). Source rocks evaluation of Sidi Salem-1 well in the onshore Nile Delta, Egypt. *Petroleum Science and Technology, 28*, 1492–1502.

El-Hawat, A. S., Missallati, A. A., Bezan, A. M., Taleb, T. M. (1997). The Nubian sandstone in Sirt Basin and its correlatives. In M. J. Salem, A. J. Mouzughi, O.S. Hammda (Eds.), *The geology of Sirt Basin* (vol. 2, pp. 3–30). Elsevier

El-Soughier, M. I., Mahmoud, M. S., & Li, J. (2010). Palynology and palynofacies of the lower cretaceous succession of the Matruh 2-1X borehole, Northwestern Egypt. *Revista Española De Micropaleontología, 42*, 37–58.

Felestteen, A. W., El-Soughier, M. I., Mohamed, M. S., & Monged, M. N. S. (2014). Hydrocarbon source potential of the Jurassic sediments of Salam-3X borehole, Khalda Concession, Northern Western Desert, Egypt. *Arabian Journal of Geosciences, 7*, 3467–3480.

Galloway, W. E. (1975). Process framework for describing the morphologic and stratigraphic evolution of deltaic depositional systems. In M. L. Broussard (Ed.), *Deltas: Models for exploration* (pp. 87–98). Houston Geological Society

Gentzis, T., Carvajal-Ortiz, H., Deaf, D., & Tahoun, S. S. (2018). Multi-proxy approach to screen the hydrocarbon potential of the Jurassic succession in the Matruh Basin, North Western Desert, Egypt. *International Journal of Coal Geology, 190*, 29–41.

Ghassal, B., Littke, R., El Atfy, H., Sindern, S., Scholtysik, G., El Beialy, S., & El Khoriby, E. (2018). Source rock potential and depositional environment of upper cretaceous sedimentary rocks, Abu Gharadig Basin, Western Desert, Egypt: An integrated palynological, organic and inorganic geochemical study. *International Journal of Coal Geology, 186*, 14–40.

Ghassal, B. I. (2010). Petroleum geochemistry and geology of the Midyan and Al Wajah Basins, northern Red Sea, Saudi Arabia (p. 231). M.Sc. Thesis, The University of Utah

Ghassal, B. I., El Atfy, H., Sachse, V., & Littke, R. (2016). Source rock potential of the middle Jurassic to middle Pliocene, Onshore Nile Delta Basin, Egypt. *Arabian Journal of Geosciences, 9*, 744.

Ghassal, B. I. H. (2017). Source rock depositional processes in different marine settings: Examples from North African basins. Ph.D. Thesis, Universitätsbibliothek der RWTH Aachen. http://publications.rwth-aachen.de/record/696615/files/696615.pdf

Gluyas, J., & Swarbrick, R. (2013). *Petroleum geoscience*. Wiley.

Grohmann, S., Fietz, S. W., Littke, R., Daher, S. B., Romero-Sarmiento, M. F., Nader, F. H., Baudin, F. (2018). Source rock characterization of Mesozoic to Cenozoic organic matter rich marls and shales of the Eratosthenes Seamount, Eastern Mediterranean Sea. *Oil & Gas Science and TechnologyRevue d'IFP Energies nouvelles, 73*, 49

Guiraud, R., Bellion, Y., Benkhelil, J., & Moreau, C. (1987). Post-Hercynian tectonics in Northern and Western Africa. *Geological Journal, 22*, 433–466.

Guiraud, R., & Bosworth, W. (1999). Phanerozoic geodynamic evolution of northeastern Africa and the northwestern Arabian platform. *Tectonophysics, 315*, 73–108.

Guiraud, R., Bosworth, W., Thierry, J., & Delplanque, A. (2005). Phanerozoic geological evolution of Northern and Central Africa: An overview. *Journal of African Earth Sciences, 43*, 83–143.

Haq, B. U., Hardenbol, J., Vail, P. R. (1988). Mesozoic and Cenozoic chronostratigraphy and cycles of sea-level changes. In C. K. Wilgus, B. S. Hastings, H. W. Posamentier, J. van Wagoner, C. A. Ross, Kendall G. S. C. (Eds.), *Sea-level changes: An integrated approach* (pp. 71–108). Society of Economic Paleontologists and Mineralogists, Special Publication no. 42.

Hartkopf-Fröder, C., Königshof, P., Littke, R., & Schwarzbauer, J. (2015). Optical thermal maturity parameters and organic geochemical alteration at low grade diagenesis to anchimetamorphism: A review. *International Journal of Coal Geology, 150–151*, 74–119.

Hewaidy, A. A., Baioumi, A., Makled, W. A., El Garhy M. M. (2014). Integrated palynological and organic geochemical analysis of Jurassic rocks from BYX-1 Borehole, North Western Desert, Egypt. *Egyptian Journal of Paleontology, 14*, 157–188

Ibrahim, M. I. A. (1996). Spore colour index and organic thermal maturation studies on the Pliocene sediments of the El Qara-2 borehole, Nile Delta, Egypt. *Qatar University Science Journal, 16* (1), 167–172.

Ibrahim, M. I. A., Aboul Ela, N. M., & Kholeif, S. E. (1997). Paleoecology, palynofacies, thermal maturation and hydrocarbon source-rock potential of the Jurassic-lower cretaceous sequence in the subsurface of the north Eastern Desert, Egypt. *Qatar University Science Journal, 17*(1), 153–172.

Jenkyns, H. C. (2010). Geochemistry of oceanic anoxic events. *Geochemistry, Geophysics, Geosystems, 11*(3), 1–30.

Katz, B. (2012). *Petroleum source rocks*. Springer Science & Business Media

Katz, B, J. (1995). Petroleum source rocks—an introductory overview. In B. J. Katz (Ed.), *Petroleum source rocks* (pp. 1–8). Springer

Keeley, M. L. (1989). The Palaeozoic history of the Western Desert of Egypt. *Basin Research, 2*, 35–48.

Keshta, S., Metwalli, F. J., Al Arabi, H. S. (2012). Analysis of petroleum system for exploration and risk reduction in Abu Madi/Elqar'a Gas Field, Nile Delta, Egypt. *International Journal of Geophysics*. https://doi.org/10.1155/2012/187938

Klitzsch, E. (1990). Paleozoic. In R. Said (Ed.), *Geology of Egypt* (pp. 393–406). A.A Balkema/Rotterdam/Brookfield

Koblentz-Mishke, O. J., Volkovinsky. V. V., Kabanova, J. G. (1970). Plankton primary production of the World Ocean. In W. S. Wooster (Ed.), *Scientific exploration of the South Pacific* (pp. 183–193)

Littke, R. (1993). Deposition, diagenesis and weathering of organic matter-rich sediments. In *Lecture Notes in Earth Sciences* (p. 216). Springer

Littke, R., Baker, D. R., Rullkötter, J. (1997). Deposition of petroleum source rocks. In D. H. Welte, B. Horsfield, D. R. Bake (Eds.), *Petroleum and basin evolution* (pp. 271–333). Springer

Lučić, D., & Bosworth, W., et al. (2019). Regional geology and petroleum systems of the main reservoirs and source rocks of North Africa and the Middle East. In A. Bendaoud (Ed.), *The geology of the Arab world—An overview* (pp. 197–289). Springer.

Lüning, S., Craig, J., Loydell, D. K., Storch, P., & Fitches, B. (2000). Lowermost Silurian 'hot shales' in north Africa and Arabia: Regional distribution and depositional model. *Earth Science Reviews, 49*, 121–200.

Mahmoud, M. S., Deaf, A. S., Tamam, M. A., & Khalaf, M. M. (2017). Palynofacies analysis and palaeoenvironmental reconstruction of the upper cretaceous sequence drilled by the Salam-60 well, Shushan Basin: Implications on the regional depositional environments and hydrocarbon exploration potential of North-Western Egypt. *Revue De Micropaléontologie, 60*, 449–467.

Makled, W. A., Mostafa, T. F., Mousa, D. A., & Abdou, A. A. (2018). Source rock evaluation and sequence stratigraphic model based on the palynofacies and geochemical analysis of the subsurface Devonian rocks in the Western Desert, Egypt. *Marine and Petroleum Geology, 89*, 560–584.

Makled, W. A., Gentzis, A., Hosny, A. M., Mousa, D. A., Lotfy, M. M., Abd El Ghany, A. A., El Sawy, M. Z., Orabi, A. A., Abdelrazak, H. A., & Shahat, W. A. (2021). Depositional dynamics of the Devonian rocks and their influence on the distribution patterns of liptinite in the Sifa-1X well, Western Desert, Egypt: Implications for hydrocarbon generation. *Marine and Petroleum Geology, 126*, 104935.

Mansour, A., Geršlová, E., Sýkorová, I., & VoRoš, D. (2020). Hydrocarbon potential and depositional paleoenvironment of a Middle Jurassic succession in the Falak-21 well, Shushan Basin, Egypt: Integrated palynological, geochemical and organic petrographic approach. *International Journal of Coal Geology, 19*, 103374.

Marshall, J. E. A., & Yule, B. L. (1999). Spore colour measurement. In T. P. Jones & N. P. Rowe (Eds.), *Fossil plants and spores: Modern techniques* (pp. 165–168). Geological Society.

Mostafa, A. R., & Ganz, H. (1990). Source rock evaluation of a well in the Abu Rudeis area, Gulf of Suez. *Berliner Geowissenschaftliche Abhandlungen, 120*, 1027–1040.

Parrish, J. T. (1987). Palaeo-upwelling and the distribution of organic-rich rocks. *Geological Society, London, Special Publications, 26*(1), 199–205.

Pearson, D. L. (1984). Pollen/spore color "standard". Phillips petroleum company exploration projects section (reproduction in traverse 2007). In *Paleopalynology*, Figure 19.2. Springer

Peters, K. E., Snedden, J. W., Sulaeman, A., Sarg, J. F., & Enrico, R. J. (2000). A new geochemical sequence Stratigraphic model for Mahakam Delta and Makassar slope, Kalimantan, Indonesia. *AAPG Bulletin, 84*, 12–44.

Ryther, J. H. (1969). Photosynthesis and fish production in the sea: The production of organic matter and its conversion to higher forms of life vary throughout the world ocean. *Science, 166*(3901), 72–76

Selley, R. C. (1998). *Elements of petroleum geology* (2nd ed., p.470). Academic Press

Shaaban, F., Lutz, R., Littke, R., Bueker, C., & Odisho, K. (2006). Source-rock evaluation and basin modelling in ne Egypt (NE Nile Delta and northern Sinai). *Journal of Petroleum Geology, 29*, 103–124.

Tissot, B., & Welte, D. H. (1984). *Petroleum formation and occurrence* (p. 699). Springer.

Tuttle, M. L. W., Charpentier, R. R., Brownfield, M. E. (1999). The Niger delta petroleum system: Niger Delta Province, Nigeria, Cameroon, and Equatorial Guinea, Africa. U.S. Geological Survey, Open-File Report 99-50-H

Tyson, R. V. (1995). *Sedimentary organic matter—organic facies and palynofacies* (p. 615). Chapman and Hall.

Yahi, A., Schaefer, R. G., & Littke, R. (2001). Petroleum generation and accumulation in the Berkine basin, eastern Algeria. *AAPG Bulletin, 85*(8), 1439–1467.

Zobaa, M. K., El Beialy, S. Y., El-Sheikh, H. A., & El Beshtawy, M. K. (2013). Jurassic-Cretaceous palynomorphs, palynofacies, and petroleum potential of the Sharib-1X and Ghoroud-1X wells, North Western Desert, Egypt. *Journal of African Earth Sciences, 78*, 51–65.

Zobaa, M. K., Oboh-Ikuenobe, F. E., & Ibrahim, M. I. I. (2011). The Cenomanian/Turonian oceanic anoxic event in the Razzak Field, north Western Desert, Egypt: Source rock potential and paleoenvironmental association. *Marine and Petroleum Geology, 28*, 1475–1482.

Haytham El Atfy is an associate professor at Mansoura University (Egypt) from where he received a BSc degree in geology and an MSc in palynology. He received a PhD in geosciences (palynology and organic geochemistry) from Goethe University, Frankfurt (Germany) in 2014, and acquired experience in industrial palynology through work with GUPCO (BP), Egypt. Haytham has been a Research Fellow of the Alexander von Humboldt Foundation at the University of Tübingen (Germany) since 2019. He was recently a visiting scientist at the Senckenberg Research Institute, Germany. His research interests span all aspects of palynology and its applications in dating, palaeoenvironmental and palaeoclimatical reconstructions, and hydrocarbon exploration, particularly of the Mesozoic and Cenozoic and, to a lesser extent, the Palaeozoic. He has more recently become involved in organic geochemistry. He is a member of the AASP – The Palynological Society, the Micropalaeontological Society (TMS), Arbeitskreis für Paläobotanik und Palynologie (APP), and the Paleontological Society of Egypt (PSE). He is a recipient of many awards, including the Bernd Rendel Prize from the German Science Foundation (DFG), Egyptian State Incentive Award, and the First-Class Excellence Concession that is provided by the Egyptian president.

Bandar I. Ghassal is a petroleum geochemist and supervisor at the Saudi Aramco EXPEC Advanced Research Center. He has 17 years of industry and academic experience in mineral resource and petroleum exploration fields. He obtained a BSc (2004) degree from King Abdulaziz University (Saudi Arabia), MSc (2010) from the University of Utah (USA), and a PhD (2017) from RWTH Aachen University, Germany. He has published several papers on various topics in petroleum geology and engineering.

Ralf Littke has been a professor of geology and geochemistry of petroleum and coal at RWTH Aachen University (Germany) since 1997. He graduated with a BSc degree in geology from Ruhr-University Bochum (Germany), where he also received his PhD degree in 1985 and Habilitation in 1993. From 1985 to 1997, he worked at the Federal Research Center Jülich, Germany, in the Institute of Petroleum and Organic Geochemistry. His research interests include (1) dynamics and numerical modeling of sedimentary basins, (2) generation and storage of oil and natural gas, (3) transport and accumulation of petroleum fluids, (4) geology, petrology and geochemistry of petroleum source rocks and coals, and (5) unconventional fossil fuels. He is a member of the German National Academy of Science and Engineering (Acatech) and member of the Academy of Sciences and Arts, Northrhine-Westfalia. He is also a former chairman of the Board of Geologische Vereinigung (German Geological Union), former chairman of the Advisory Board of Deutsches Geoforschungszentrum (GFZ Potsdam), longtime editor-in-chief of International Journal of Coal Geology, and former coordinator of the German priority research program Dynamics of Sedimentary Basins.